https://doi.org/10.5194/acp-2019-1209
Preprint. Discussion started: 4 February 2020

Atmospheric Chemistry and Physics Discussions

Climate and air quality impacts due to mitigation of non-methane near-term climate forcers

Robert J. Allen[1], Steven Turnock[2], Pierre Nabat[3], David Neubauer[4], Ulrike Lohmann[4], Dirk Olivie[5], Naga Oshima[6], Martine Michou[3], Tongwen Wu[7], Jie Zhang[7], Toshihiko Takemura[8], Michael Schulz[5], Kostas Tsigaridis[9], Susanne E. Bauer[9], Louisa Emmons[10], Larry Horowitz[11], Vaishali Naik[11], Twan van Noije[12], Tommi Bergman[12,13], Jean-Francois Lamarque[14], Prodromos Zanis[15], Ina Tegen[16], Daniel M. Westervelt[17], Phillipe Le Sager[12], Peter Good[2], Sungbo Shim[18], Fiona O'Connor[2], Dimitris Akritidis[15], Aristeidis K. Georgoulias[15], Makoto Deushi[6], Lori T. Sentman[11], Shinichiro Fujimori[19,20,21], and William J. Collins[22]

[1]Department of Earth and Planetary Sciences, University of California Riverside, Riverside, CA, 92521 USA
[2]Met Office Hadley Centre, Exeter, UK
[3]Centre National de Recherches Meteorologiques (CNRM), Universite de Toulouse, Meteo-France, CNRS, Toulouse, France
[4]Institute of Atmospheric and Climate Science, ETH Zurich, Zurich, Switzerland
[5]Norwegian Meteorological Institute, Oslo, Norway
[6]Meteorological Research Institute, Japan Meteorological Agency
[7]Beijing Climate Center, China Meteorological Administration, Beijing, China
[8]Research Institute for Applied Mechanics, Kyushu University, Fukuoka, Japan
[9]Center for Climate Systems Research, Columbia University, NASA Goddard Institute for Space Studies, USA
[10]Atmospheric Chemistry Observations and Modelling Lab, National Center for Atmospheric Research, Boulder, CO, USA
[11]DOC/NOAA/OAR/Geophysical Fluid Dynamics Laboratory. Biogeochemistry, Atmospheric Chemistry, and Ecology 10 Division, Princeton, USA
[12]Royal Netherlands Meteorological Institute, De Bilt, Netherlands
[13]Finnish Meteorological Institute, Helsinki, Finland
[14]NCAR/UCAR, Boulder, CO, USA
[15]Department of Meteorology and Climatology, School of Geology, Aristotle University of Thessaloniki, Thessaloniki, Greece
[16]Leibniz Institute for Tropospheric Research, Leipzig, Germany
[17]Lamont-Doherty Earth Observatory, Columbia University, Palisades, New York, USA
[18]National Institute of Meteorological Sciences, Seogwipo-si, Jeju-do, Korea
[19]Department of Environmental Engineering, Kyoto University, C1-3 361, Kyotodaigaku Katsura, Nishikyoku, Kyoto city, Japan
[20]Center for Social and Environmental Systems Research, National Institute for Environmental Studies (NIES), 16-2 Onogawa, Tsukuba, Ibaraki, 305-8506, Japan
[21]International Institute for Applied System Analysis (IIASA), Schlossplatz 1, A-2361, Laxenburg, Austria
[22]Department of Meteorology, University of Reading, Reading, RG6 6BB, UK

Correspondence: Robert J. Allen (rjallen@ucr.edu)

Abstract. Over the next few decades, policies that optimally address both climate change and air quality are essential. Although targeting near-term climate forcers (NTCFs), defined here as aerosols, tropospheric ozone and precursor gases (but not methane), should improve air quality, NTCF reductions will also impact climate. How future policies affect the abundance of NTCFs and their impact on climate and air quality remains uncertain. Here, we quantify the 2015-2055 climate and air qual-

https://doi.org/10.5194/acp-2019-1209
Preprint. Discussion started: 4 February 2020

Atmospheric Chemistry and Physics Discussions

ity effects of non-methane NTCFs using state-of-the-art chemistry-climate model simulations conducted for the Aerosol and Chemistry Model Intercomparison Project (AerChemMIP). Simulations are driven by two future scenarios featuring similar increases in greenhouse gases (GHGs) but with “weak" versus “strong" levels of air quality control measures. Unsurprisingly, we find significant improvements in air quality under NTCF mitigation (strong versus weak air quality controls). Surface ozone (O_3) and fine particulate matter ($PM_{2.5}$) decrease by -15% and -25%, respectively, over global land surfaces, with larger reductions in some regions including south and southeast Asia. Non-methane NTCF mitigation, however, leads to additional climate change due to the removal of aerosol which causes a net warming effect, including global mean surface temperature and precipitation increases of 0.24K and 1.1%, respectively, with similar increases in extreme weather indices. Regionally, the largest warming and wetting trends occur over Asia, including central and north Asia (0.56K and 2.1%), south Asia (0.48K and 4.6%) and east Asia (0.44K and 4.7%). Relatively large warming and wetting of the Arctic also occurs at 0.41K and 2.1%, respectively. Similar surface warming occurs in model simulations with aerosol-only mitigation, implying weak cooling due to ozone reductions. Our findings suggest that future policies that aggressively target non-methane NTCF reductions will improve air quality, but will lead to additional surface warming, particularly in Asia and the Arctic. Policies that address other NTCFs including methane, as well as carbon dioxide emissions, must also be adopted to meet mitigation goals.

1 Introduction

Near-term climate forcers (NTCFs) are compounds that impact climate on relatively short time scales, typically within a few weeks to a decade after emission (Myhre et al., 2013). This set of compounds includes ozone, aerosols, and their precursor gases, as well methane (CH_4) which is also a well-mixed greenhouse gas (GHG). Other well-mixed GHGs, including carbon dioxide (CO_2) and nitrous oxide (N_2O), possess much longer atmospheric lifetimes, are sufficiently mixed throughout the troposphere, and impact climate on decadal to centennial time scales.

NTCFs have important impacts on the climate system and human health, as they perturb the radiative balance of the planet and contribute to air pollution. The total aerosol radiative effect, estimated as an effective radiative forcing (ERF), is -0.9 W m^{-2} with a 90% confidence range of -1.9 to -0.1 W m^{-2} (Boucher et al., 2013). A more recent review revised the 90% confidence range to more negative values (-0.4 to -2.0 W m^{-2}) (Bellouin et al., in press). Moreover, not all aerosols have a negative forcing, as black carbon (BC) from anthropogenic fossil and biofuel emissions possesses a forcing of +0.40 (0.05 to 0.80) W m^{-2}. BC, however, is always associated with organic carbon (OC), the net radiative effect being slightly negative but with relatively large uncertainty bounds of -1.45 to +1.29 W m^{-2} (Bond et al., 2013). Thus, changes in BC emissions that are different from changes in non-absorbing aerosols will lead to differing ERF changes. Tropospheric ozone, which is formed in the atmosphere through photochemical reactions with nitrogen oxides (NO_x), carbon monoxide (CO) and volatile organic compounds (VOCs), also exhibits a positive forcing of +0.40$\pm$0.2 W m^{-2} (Myhre et al., 2013). Similarly, the radiative forcing of methane emissions, including secondary effects like its ability to act as a precursor to tropospheric ozone, is estimated at +0.97$\pm$0.23 W m^{-2} (Myhre et al., 2013). We note that these estimates are currently being updated as part of the Radiative Forcing Model Intercomparison Project (RFMIP) (Pincus et al., 2016). Thus, reductions in some NTCFs,

https://doi.org/10.5194/acp-2019-1209
Preprint. Discussion started: 4 February 2020


Atmospheric Chemistry and Physics Discussions

including non-absorbing aerosols, will warm the climate system, whereas reductions in other NTCFs, including absorbing aerosols, tropospheric ozone, and methane will cool the climate system.

NTCFs also perturb the hydrological cycle. Energetic constraints and modeling studies show that anthropogenic aerosols lead to reduced global mean precipitation (Ramanathan et al., 2001; Wilcox et al., 2013; Samset et al., 2016). Aerosol induced reductions in surface solar radiation will be partially balanced by reductions in evaporation, leading to corresponding rainfall reductions. In the case of absorbing aerosols—particularly in the boundary layer—atmospheric heating stabilizes the atmosphere and reduces convection, also leading to an overall decrease in precipitation (Ming et al., 2010; Ban-Weiss et al., 2012; Stjern et al., 2017; Allen et al., 2019a; Johnson et al., 2019). The buildup of aerosols during the 20th century has likely masked the expected increase in global mean precipitation due to GHGs (Liepert et al., 2004; Wu et al., 2013; Salzmann, 2016; Richardson et al., 2018). Furthermore, the hemispheric contrast in aerosol forcing has likely shifted the tropical rainbelt southward, which is associated with a weakening of the west African Monsoon and the occurrence of the Sahel drought of the mid-1980s (Rotstayn and Lohmann, 2002; Biasutti and Giannini, 2006; Allen and Sherwood, 2011; Ackerley et al., 2011; Chang et al., 2011; Biasutti, 2013; Hwang et al., 2013; Dong et al., 2014; Allen et al., 2015; Undorf et al., 2018). The observed precipitation decrease during recent decades over most of the areas affected by the South and East Asia monsoon can also be explained by the dominance of aerosol radiative effects suppressing precipitation over the expected precipitation enhancement due to increased GHGs (Wang et al., 2013; Song et al., 2014; Li et al., 2015; Xie et al., 2016; Krishnan et al., 2016; Guo et al., 2016; Lau and Kim, 2017; Zhang et al., 2017; Lin et al., 2018; Liu et al., 2018).

NTCFs are also a source of air pollution, including surface ozone (O_3) and fine particulate matter less than 2.5 μm in diameter ($PM_{2.5}$). Air pollution has negative impacts on human health, including exacerbation of cardiovascular and respiratory diseases, and cancer. Recent estimates show air pollution is the 4th highest ranking risk factor for death globally, responsible for $\sim$7 million premature deaths per year, with 4.2 million of these annual deaths attributable to ambient air pollution (WHO, 2016; Cohen et al., 2017; Butt et al., 2017). A more recent study suggests the global total excess mortality rate is 8.79 million per year (95% confidence interval of 7.11-10.41 million per year), leading to a global mean loss of life expectancy of 2.9 years (Lelieveld et al., 2019).

Future reductions in NTCF emissions are necessary for improved air quality, but will likely yield rapid climate responses due to their short atmospheric lifetimes (relative to GHGs). Samset et al. (2018) show that complete removal of present-day anthropogenic aerosol emissions induces a global mean surface heating of 0.5-1.1K and a precipitation increase of 2-4.6%. Similar large, near-term increases in global warming and precipitation are predicted by other studies that assume a rapid removal of anthropogenic aerosols (Brasseur and Roeckner, 2005; Andreae et al., 2005; Ramanathan and Feng, 2008; Raes and Seinfeld, 2009; Kloster et al., 2010; Arneth et al., 2009; Matthews and Zickfeld, 2012; Rotstayn et al., 2013; Wu et al., 2013; Westervelt et al., 2015; Salzmann, 2016; Hienola et al., 2018; Richardson et al., 2018; Lelieveld et al., 2019). Furthermore, future aerosol reductions will likely shift the tropical rainbelt northward and may strengthen precipitation in several monsoon regions, including West Africa, South Asia, and East Asia (Levy et al., 2013; Allen, 2015; Rotstayn et al., 2015; Allen and Ajoku, 2016; Westervelt et al., 2017; Zhao et al., 2018; Westervelt et al., 2018; Scannell et al., submitted; Zanis et al., submitted). In contrast to the above studies, however, Shindell and Smith (2019) show that the time required to

https://doi.org/10.5194/acp-2019-1209
Preprint. Discussion started: 4 February 2020

Atmospheric Chemistry and Physics Discussions

transform power generation, industry and transportation leads to largely offsetting climate impacts of CO_2 and sulfur dioxide (a precursor of sulfate aerosol), implying no conflict between climate and air-quality objectives. Their simulations use a simple emissions-based climate model, Finite Amplitude Impulse Response (FAIR) (Smith et al., 2018), and it is not known if this result also applies to fully coupled chemistry-climate models.

Despite the rich literature, the impact of NTCF mitigation on climate and air quality remains uncertain. Part of this uncertainty stems from the idealized nature of many of the prior studies (e.g., instantaneous removal of all aerosols), simplified treatment of aerosols and chemically reactive gases, as well as a lack of a sufficiently large number of models performing identical simulations with which to quantify model diversity and robust responses. The Aerosol and Chemistry Model Intercomparison Project (AerChemMIP) (Collins et al., 2017), part of the Coupled-Model Intercomparison Project 6 (CMIP6) (Eyring et al., 2016) quantifies the climate and air quality impacts of aerosols and chemically reactive gases. Here, we use AerChemMIP simulations to quantify the climate and air quality impacts due to non-methane NTCF mitigation (aerosols and ozone only). Models include an interactive representation of tropospheric aerosols and atmospheric chemistry, allowing for the quantification of chemistry-climate interactions. We show that non-methane NTCF reductions improve air quality, but also lead to additional climate change including surface warming. Policies that address other NTCFs including CH_4, as well as CO_2 emissions, must also be undertaken. Methods are presented in Section 2 and results are discussed in Section 3. Conclusions appear in Section 4.

2 Methods

2.1 Future Scenarios: SSP3-7.0 and SSP3-7.0-lowNTCF

Future scenarios are based on the Shared Socio-economic Pathways (SSPs) (O'Neill et al., 2014; van Vuuren et al., 2014; Gidden et al., 2019), which include representations of different levels of controls on air pollutants. The medium strength of pollution control corresponds to current legislation (CLE) until 2030 and progresses three-quarters of the way towards maximum technically feasible reduction (MTFR) thereafter. Strong pollution control exceeds CLE and progresses ultimately towards MTFR. Weak pollution control assumes delays to the implementation of CLE and makes less progress towards MTFR than the medium scenario (Rao et al., 2017). The rate of progress is different for high, medium and low-income countries.

The reference scenario used here is SSP3-7.0 "Regional Rivalry" without climate policy ($\sim$7.0 W m^{-2} at 2100) (Fujimori et al., 2017), which has the highest levels of NTCFs and "weak" levels of air quality control measures (O'Neill et al., 2014; Rao et al., 2017). The perturbation scenario SSP3-7.0-lowNTCF uses the same socio-economic scenario, but with "strong" levels of air quality control measures (Gidden et al., 2019). Basically, the emissions drivers (population, GDP, energy and land-use) are based on SSP3, but the emissions factors are associated with a Sustainability pathway represented by SSP1. Differences in climate, effective radiative forcing, chemical composition and air quality between the two scenarios will be solely due to the alternative air quality control measures. These experiments cover the time frame from 2015 to 2055, as this is when reductions in aerosol and ozone precursor emissions are expected to be significant, particularly in some world regions. Here, we define NTCF mitigation as the difference between the weak (high NTCF) and strong (low NTCF) air quality control scenarios

https://doi.org/10.5194/acp-2019-1209
Preprint. Discussion started: 4 February 2020

Atmospheric Chemistry and Physics Discussions

(i.e., SSP3-7.0-lowNTCF minus SSP3-7.0). Although methane reductions are included in SSP3-7.0-lowNTCF, AerChemMIP protocol specifies unchanged levels of WMGHGs, including methane, between the strong and the weak air quality control simulations (Collins et al., 2017). Thus, our results quantify non-methane NTCF mitigation (aerosols and ozone only).

2.2 AerChemMIP Models

Eight coupled ocean-atmosphere climate models performed the SSP3-7.0 and SSP3-7.0-lowNTCF simulations, including CNRM-ESM2-1 (Séférian et al., 2019; Michou et al., 2019), MIROC6 (Takemura et al., 2005, 2009; Tatebe et al., 2019), MPI-ESM1-2-HAM (Mauritsen et al., 2019; Neubauer et al., 2019; Tegen et al., 2019), BCC-ESM1 (Wu et al., 2019, submitted), GFDL-ESM4 (Dunne and et al., In prep.; Horowitz and et al., In prep.), CESM2-WACCM and CESM2 (Emmons et al., submitted, 2019; Gettelman et al., in press; Tilmes et al., in press), and MRI-ESM2-0 (Yukimoto et al., 2019). However, the first three models (CNRM-ESM2-1, MIROC6, MPI-ESM1-2-HAM) lack interactive tropospheric chemistry schemes and therefore include identical ozone evolution in both SSP3-7.0 and SSP3-7.0-lowNTCF simulations (as recommended by AerChemMIP). As NTCF mitigation only includes the effects of aerosols in these three models, we refer to these models as “lowAER". The remaining five models, including BCC-ESM1, GFDL-ESM4, CESM2-WACCM, CESM2, and MRI-ESM2-0, include interactive atmospheric chemistry and aerosols, and therefore both aerosol and ozone reductions are included. These models are referred to as “lowAERO3". In the case of CESM2, which we include in lowAERO3, ozone changes are based on CESM2-WACCM. Thus, although CESM2 lacks interactive tropospheric chemistry, its SSP3-7.0-lowNTCF simulation includes changes in ozone as simulated by CESM2-WACCM.

In addition to coupled simulations, models also performed analogous fixed SST experiments to quantify the effective radiative forcing (ERF). The ERF is calculated from the top-of-the-atmosphere (TOA) flux differences between atmosphere-only simulations with identical SSTs but differing composition (Forster et al., 2016; Pincus et al., 2016). The above scenarios (SSP3-7.0 and SSP3-7.0-lowNTCF) are repeated with prescribed SSTs. These SSTs (and sea ice) are taken from the monthly mean evolving values from one ensemble member of the coupled SSP3-7.0 run. MPI-ESM1-2-HAM used daily mean SST and sea ice. The differences in radiative fluxes between the high and low NTCF simulation yields the TOA transient ERF due to NTCF mitigation.

2.3 Model Data and Methodology

All models performed at least one realization of SSP3-7.0 and SSP3-7.0-lowNTCF. CNRM-ESM2-1, MIROC6 and BCC-ESM1 performed three realizations of each experiment. For these models, the model mean response (average over the three realizations) is shown. The multi-model mean (MMM) is obtained by averaging each model’s mean response. Only one realization exists for the corresponding fixed SST experiments. Unless otherwise mentioned, all analyses are based on annual means. All data is spatially re-interpolated to a 2.5°x2.5° grid using bilinear interpolation. Trends are calculated using least squares regression, and the corresponding trend significance is based on a standard t-test.

Climate variables analyzed include monthly mean surface temperature (Ts) and precipitation (Precip). Air quality is quantified from surface $PM_{2.5}$ and surface O_3. These monthly mean fields are obtained from the model level closest to the surface.

https://doi.org/10.5194/acp-2019-1209
Preprint. Discussion started: 4 February 2020

Atmospheric Chemistry and Physics Discussions

Unfortunately, few models archived sub-monthly aerosol or ozone data, so were are unable to analyze changes in daily or sub-daily maximum $PM_{2.5}$ or O_3 pollution. Furthermore, few models directly archive $PM_{2.5}$ for SSP3-7.0 and SSP3-7.0-lowNTCF (GFDL-ESM4 is the lone model), and not all models include the same aerosol species (e.g., nitrate aerosol). Thus, we approximate $PM_{2.5}$ in all models using the following equation (Fiore et al., 2012; Silva et al., 2017): $PM_{2.5}$ = BC + OA + SO_4 + 0.1xDU + 0.25xSS, where BC is black carbon, OA is organic aerosol, SO_4 is sulfate aerosol, DU is dust and SS is sea salt. This formula assumes 100% of the BC, OA and SO_4 is fine mode, whereas 25% of the sea salt and 10% of the dust is fine mode. The SS and DU factors are likely dependent on the model and its size distribution. In the case of CNRM-ESM2-1, sensitivity tests were used to estimate a much smaller SS factor of 0.01. This smaller factor addresses the large SS size range of up to 20 μm in this model (P. Nabat 2019, personal communication, November 27th). Although this approach likely introduces some uncertainties, it provides first and foremost an estimate of $PM_{2.5}$ for all models, as well as a consistent estimate for all models.

CMIP6 model evaluation of air quality metrics, including surface O_3 and $PM_{2.5}$ (as approximated here) is quantified in a companion paper (Turnock et al., submitted). To summarize, CMIP6 models generally underestimate $PM_{2.5}$ over most regions relative to ground based observations from the Global Aerosol Synthesis and Science Project (GASSP) (Reddington et al., 2017). This in part is due to the absence of nitrate aerosol, and may also be related to misrepresentation of secondary organic aerosol. A similar $PM_{2.5}$ underestimation occurs over Europe and North America relative to the Modern-Era Retrospective Analysis for Research and Applications, version 2 (MERRA2) aerosol reanalysis product (Buchard et al., 2017; Randles et al., 2017). In contrast, CMIP6 models overestimate $PM_{2.5}$ relative to MERRA2 over south and east Asia, contrary to the evaluation using ground based observations. Compared to surface O_3 measurements from Tropospheric Ozone Assessment Report (TOAR) (Schultz et al., 2017), CMIP6 models consistently overestimate surface ozone during both summer and winter across most regions, potentially due to the coarse resolution of global models simulating excess O_3 production.

We also analyze climate extremes based on daily data, including the hottest day (monthly maximum value of daily maximum temperature), wettest day (monthly maximum 1-day precipitation) and consecutive dry days (CDD), defined as the maximum annual number of consecutive days with precipitation < 1 mm day^{-1} (Donat et al., 2013a, b). Climate extremes are calculated at each grid box, and then spatially averaged.

3 Results

3.1 SSP3-7.0 and SSP3-7.0-lowNTCF Emissions

Figure 1 shows the 2015-2055 global mean time series of CO_2, CH_4, aerosol species and gaseous precursor emissions for SSP3-7.0 (weak air quality control) and SSP3-7.0-lowNTCF (strong air quality control). Under both scenarios, CO_2 emissions similarly increase. By 2055, CO_2 increases by 65-70% (relative to 2015), with a very small ($\sim$3%) difference between weak and strong air quality control pathways. However, very different NTCF evolution occurs. Under weak air quality control, global emissions of all aerosols and gaseous precursors (except SO_2) increase by 5-15% by 2055 (relative to 2015). In contrast, strong air quality control yields strong emission reductions in all species, ranging from $\sim$30% for VOCs to 55% for SO_2. Thus, NTCF mitigation (SSP3-7.0-lowNTCF$-$SSP3-7.0) yields emission reductions of all aerosols and gaseous precursors by $\sim$40-55%.

https://doi.org/10.5194/acp-2019-1209
Preprint. Discussion started: 4 February 2020

Atmospheric Chemistry and Physics Discussions

We note that large differences in CH_4 emissions also occur between the two scenarios. By 2055, CH_4 decreases by 100% under NTCF mitigation (50% increase and 50% decrease under weak and strong air quality control, respectively). Methane reduction generates emissions abatement costs which changes economic outputs in all sectors, which in turn impacts energy consumption and CO_2 emissions in all sectors, causing the aforementioned small CO_2 differences between strong and weak air quality control pathways (Gidden et al., 2019).

This difference in CH_4 emission, however, is not included in the AerChemMIP simulations analyzed here. According to the AerChemMIP protocol, levels of WMGHGs (including methane) are unchanged between the strong and the weak air quality control simulations (Collins et al., 2017). Thus, both high and low NTCF simulations include the same change in methane emissions (most models prescribe methane concentrations based on these emissions) which follow SSP3-7.0. Future studies looking at NTCF mitigation should also include the impact of reduced CH_4 emissions. As estimates of methane's total forcing are relatively large ($+0.97 \pm 0.23$ W m^{-2}), future CH_4 reductions will help offset aerosol-induced warming and have important impacts on tropospheric O_3. Reducing CH_4 is the key precursor for controlling future tropospheric O_3 increases (Turnock et al., 2019b). The Model for the Assessment of Greenhouse Gas Induced Climate Change (MAGICC) estimates a 2050 CH_4 radiative forcing of 0.73 and 0.35 W m^{-2} for weak and strong air quality control, respectively (-0.38 W m^{-2} under methane mitigation), which will offset some of the aerosol and ozone effects, if CH_4 is considered (S. Fujimori, 2019, personal communication, December 26th). Moreover, by the end century, the methane reduction effects become much stronger.

The corresponding 2015-2055 regional emission trends (relative to 2015) are shown in Figure 2. Consistent with the global mean times series of emissions (Fig. 1), CO_2 emissions similarly increase in both SSP3-7.0 (weak air quality control) and SSP3-7.0-lowNTCF (strong air quality control), with larger increases (relative to 2015) in south and north Africa, south Asia, and southeast Asia. By design, NTCF mitigation (SSP3-7.0-lowNTCF$-$SSP3-7.0) yields negligible change in CO_2 emissions for all world regions. CH_4 emissions increase in all world regions under weak air quality control and decrease in all world regions except south and north Africa under strong air quality control. However, due to the large increase in south and north Africa, these two regions feature the largest decrease in CH_4 emissions under NTCF mitigation at -45 and -42% decade^{-1}, respectively. However, as previously mentioned, these changes in CH_4 emissions are not included in the AerChemMIP simulations. Most world regions also show increases in BC, SO_2 and OC under weak air quality control, but strong decreases under strong air quality control. NTCF mitigation shows large ($\sim$20% decade^{-1}) BC decreases in central America, central and north Asia, east Asia and southeast Asia. Most world regions exhibit a 10-20% decade^{-1} reduction in SO_2 emissions under NTCF mitigation, with a large decrease in south Asia at -28% decade^{-1}. Similarly, OC and CO emissions decrease by $\sim$10-20% decade^{-1}. Relatively large OC reductions also occur in east Asia, south Asia and southeast Asia. NO_x and VOC emissions also decrease in all world regions under NTCF mitigation (although this is only a decrease relative to non-mitigated emissions for NO_x in south Asia and for VOC in east Asia).

3.2 Global Climate and Air Quality Trends

Figures 3-4 show the 2015-2055 global annual mean anomaly time series for both climate and air quality under NTCF mitigation. All models shows global annual mean surface warming in response to NTCF mitigation. Averaged over all models,

https://doi.org/10.5194/acp-2019-1209
Preprint. Discussion started: 4 February 2020

Atmospheric Chemistry and Physics Discussions

global mean surface warming is 0.06 K decade^{-1}, or 0.24 K over the 2015-2055 time period (Table 1). We note that this warming will continue past 2055, as these transient simulations have not reached radiative equilibrium. Similar conclusions exist over land only, where the multi-model mean (MMM) warming is even larger at 0.32 K over the 41 year time period (Table 1). Enhanced land warming is consistent with the land-sea warming contrast (Sutton et al., 2007; Joshi et al., 2008), which may also act to increase aerosol burden itself (Allen et al., 2016, 2019b), implying a climate change penalty to air quality. Interestingly, models that include both aerosol and ozone reductions (lowAERO3) yield slightly larger surface warming relative to the models that include aerosol reductions (lowAER) alone (0.06 versus 0.05 K decade^{-1}, respectively). Although this is not a significant difference (based on a t-test for the difference in means), it is interesting nonetheless. A relatively small sample size (8 models) combined with internal climate variability could account for this difference. These are also different models with different assumptions and parameterizations. It may also be related to model differences in the aerosol forcing (i.e., larger aerosol forcing or different climate sensitivities in lowAERO3 models). It could also be due to changes in oxidants (from reductions in O_3) reducing aerosol formation, leading to more surface warming in lowAERO3. More importantly, the larger warming in lowAERO3 (which include O_3 reductions) suggests weak surface cooling due to reductions in ozone.

Warming in response to NTCF mitigation is consistent with the corresponding increase in ERF. All but one model (BCC-ESM1) yield an increase in ERF, with a MMM of 0.40 W m^{-2} over the 41 years. Over land only, this increases to 1.0 W m^{-2}. As expected, lowAERO3 models yield a weaker increase in ERF than lowAER models, at 0.24 versus 0.68 W m^{-2}. This is consistent with ozone reductions driving a decrease in ERF in lowAERO3 models, offsetting part of the ERF increase due to aerosol reductions (Turnock et al., 2019a). However, the ERF trend difference between lowAERO3 and lowAER is inconsistent with the corresponding warming contrast between these two model subsets (recall, lowAERO3 warms more than lowAER). Recalculating the MMM surface temperature and ERF trend over models that archived both parameters yields similar conclusions. This may suggest lowAERO3 models possess a larger climate sensitivity as compared to lowAER models, or that additional coupling between the chemistry and aerosol schemes (and potential other Earth System interactions) invokes different impacts. Simulations with a single model, running both coupled and uncoupled chemistry experiments, would help isolate this effect.

All models also yield an increase in global annual mean precipitation (Table 1), with an overall MMM of 0.28% decade^{-1}. Consistent with the larger surface warming in lowAERO3 models, this model subset also yields a larger increase in global mean precipitation (0.34 versus 0.20% decade^{-1}, respectively). A similar precipitation signal generally exists over land only, although both CESM2 and CESM2-WACCM yield weak (not significant) decreases in land precipitation.

Similar, but less robust responses also occur in climate extremes, particularly those based on precipitation. Global mean increases in the surface temperature of the hottest day occur in all models. The rate of increase in the hottest day is generally larger than that based on monthly mean surface temperature. Moreover, lowAERO3 models yield a slightly larger increase than lowAER models, at 0.32 versus 0.24 K from 2015-2055 respectively. Global mean precipitation extremes, including the wettest day and CDD, also increase in the overall MMM at 1.24% and 0.28% (the increase in CDD is actually a smaller decrease in SSP3-7.0-lowNTCF relative to SSP3-7.0). These responses are once again larger in lowAERO3, relative to lowAER.

https://doi.org/10.5194/acp-2019-1209
Preprint. Discussion started: 4 February 2020

Atmospheric Chemistry and Physics Discussions

Thus, from a global mean perspective, NTCF mitigation leads to significant climate change, including increases in surface temperature and precipitation, as well as corresponding increases in climate extremes.

Figure 4 shows that NTCF mitigation leads (by design) to significant decreases in air pollution, in terms of both surface $PM_{2.5}$ and O_3. All models yield global mean decreases in both quantities, with an overall MMM decrease of -3.3% decade^{-1} for $PM_{2.5}$ and -4.3% decade^{-1} for O_3 (Table 1). Over the 2015-2055 year time period, these rates of change correspond to global mean decreases of -13.2 and -17.2%, respectively. Similar $PM_{2.5}$ and O_3 decreases occur over land only, at -24.8% and -15.2%, respectively. Slightly larger (but not statistically significant) land only $PM_{2.5}$ reductions occur in lowAER models as compared to lowAERO3 (-28.4% versus -23.6%), but the reverse is true over both land and ocean. Note that the overall MMM for O_3 does not include lowAER models, as they yield negligible change in surface ozone (by design).

3.3 Regional Climate and Air Quality Trends

Figure 5 shows the regional climate and air pollution trends for weak (SSP3-7.0) and strong (SSP3-7.0-lowNTCF) air quality control, and the effect of NTCF mitigation (SSP3-7.0-lowNTCF$-$SSP3-7.0). We include both lowAER and lowAERO3 models in this analysis to maximize the signal to noise ratio (except for ozone changes). The aforementioned response differences between these two model subsets are generally not significant. Over all 12 world regions, significant surface warming occurs in both scenarios, due to continued increases in CO_2 (and CH_4). More importantly, NTCF mitigation also yields significant warming. Averaged over all land regions, warming is 0.08 ± 0.03 K decade^{-1}. Significant land warming also occurs over all 12 world regions, ranging from 0.05 ± 0.02 K decade^{-1} over southeast Asia to 0.14 ± 0.06 K decade^{-1} over central and north Asia. Relatively large warming also occurs over east Asia (0.11 ± 0.05 K decade^{-1}) and south Asia (0.12 ± 0.06 K decade^{-1}; see also Supplementary Figure 1). Furthermore, large warming of the Arctic occurs (0.10 ± 0.08 K decade^{-1}), particularly in the East Siberian and Beaufort Seas, north of western Canada/Alaska and around the Canadian Arctic Archipelago (Figure 6). This result is consistent with recent studies showing high Arctic sensitivity to aerosol reductions (Acosta Navarro et al., 2016; Lewinschal et al., 2019; Westervelt et al., 2019).

Regional warming is consistent with the increase in ERF, with most world regions yielding significant positive ERF trends. However, little correspondence exists between regions that warm the most and their ERF trend. This is not necessarily surprising, as forcing and response do not need to occur in the same regions. For example, central and north Asia warm the most, but there is not a particularly large increase in regional ERF. Similarly, southeast Asia warms the least, but this region features a relatively large ERF increase. Similar increases occur in the hottest day, with larger increases under strong relative to weak air quality controls. Thus, NTCF mitigation yields robust increases in both surface air temperature and the hottest day over all world regions (the lone exception is the non-significant increase in the hottest day over south America). We note that the lone area with robust cooling is the north Atlantic (around Iceland and southwest of Svalbard; Fig. 6), which may be associated with a weakening of the Atlantic Meridional Overturning Circulation (AMOC) (Delworth and Dixon, 2006; Cai et al., 2006; Menary et al., 2013; Hassan et al., In prep).

Over all land surfaces, a significant precipitation increase also occurs in both scenarios at $0.63\pm0.24\%$ decade^{-1} and $0.88\pm0.29\%$ decade^{-1} under weak and strong air quality control, respectively. Thus, NTCF mitigation also yields a significant

https://doi.org/10.5194/acp-2019-1209
Preprint. Discussion started: 4 February 2020

Atmospheric Chemistry and Physics Discussions

increase in land precipitation at 0.25±0.19% decade^{-1}. The effect of NTCF mitigation on precipitation over individual world regions, however, is generally not significant and ranges from −1.0±2.1% decade^{-1} over Australia to 1.2±0.77% decade^{-1} over east Asia. Note that some world regions exhibit decreases in precipitation under both weak and strong air quality control (e.g., central America), such that NTCF mitigation yields a weaker decrease (as opposed to an absolute increase). In addition to east Asia, a significant precipitation increase also occurs over central and north Asia (0.53±0.42% decade^{-1}) and the Arctic (0.53±0.46% decade^{-1}). Although south Asia also exhibits a relatively large increase in precipitation, it is not significant (1.14±1.29% decade^{-1}). Both south and north Africa yield precipitation increases, but the bulk of the African precipitation increase occurs over East Africa (Supplementary Figure 2). Thus, NTCF mitigation generally increases precipitation in most world regions (although, in some regions, this is a smaller decrease) but the signal is less robust than that for surface temperature. Furthermore, in agreement with prior studies (Levy et al., 2013; Westervelt et al., 2017; Zhao et al., 2018; Westervelt et al., 2018; Scannell et al., submitted), precipitation increases in several monsoon regions, including east Africa, south Asia, and east Asia.

Precipitation extremes, including the wettest day and CDD, also exhibit regional uncertainty under NTCF mitigation, with most regions lacking a robust response. Similar to the significant increases in mean precipitation, significant increases in the wettest day also occur in central and north Asia, east Asia, south Africa, and the Arctic. NTCF mitigation also yields robust CDD increases in Australia and south Africa. Robust CDD decreases occur in Canada, east Asia and the Arctic; central America features a smaller CDD increase under strong versus weak air quality control, yielding a relative (but not absolute) CDD decrease.

Consistent with increased aerosol and precursor gas emissions (Figures 1-2), air quality metrics generally show significant increases under weak air quality control, particularly O_3 where all 12 world regions exhibit an increase. In contrast, strong air quality control yields decreases in both $PM_{2.5}$ and O_3 for nearly all world regions. The overall effect of NTCF mitigation is thus a robust decrease in air pollution, in terms of both $PM_{2.5}$ and O_3, over all 12 world regions, as well as the Arctic. Over all land surfaces, the decrease is −6.2±0.8% decade^{-1}. Regionally, decreases in $PM_{2.5}$ range from −3.7±4.8% decade^{-1} over Australia (the lone region with a non-significant decrease) to −18.9±2.8% decade^{-1} in south Asia. Relatively large $PM_{2.5}$ decreases also occur over east Asia and southeast Asia at −11.1±1.9% decade^{-1} and −9.8±1.0% decade^{-1}, respectively. The relatively large $PM_{2.5}$ decreases over east Asia, southeast Asia, and south Asia is generally consistent with the relatively large reductions in aerosol species, including BC, SO_4 and OC (Figure 2).

Similar results exist for O_3, with a robust decrease over land of −3.8±0.5% decade^{-1}. Regionally, O_3 decreases range from −1.2±1.1% decade^{-1} over east Asia to −7.0±0.7% decade^{-1} over central America. Relatively large O_3 decreases also occur over southeast Asia (−6.8±0.6% decade^{-1}) and south America (−5.5±0.8% decade^{-1}), as well as north Africa (−4.9±0.7% decade^{-1}) and south Asia (−4.0±1.6% decade^{-1}). Notably, a weak O_3 decrease occurs in east Asia (−1.2±1.1% decade^{-1}), which may be related to relatively weak VOC reductions (Figure 2).

https://doi.org/10.5194/acp-2019-1209
Preprint. Discussion started: 4 February 2020

Atmospheric Chemistry and Physics Discussions

3.4 Seasonal Climate and Air Quality Trends

Figure 7 shows the regional surface temperature, precipitation and air quality responses during June-July-August (JJA) and December-January-February (DJF). NTCF mitigation yields warming in both seasons, with larger and more robust warming during JJA (see also Supplementary Figures 3-4). Over all land surfaces, JJA warming is 0.09 ± 0.03 K decade^{-1}; DJF warming is 0.07 ± 0.05 K decade^{-1}. Consistent with the annual mean warming, relatively large JJA warming also occurs in central and north Asia (0.14 ± 0.06 K decade^{-1}), south Asia (0.11 ± 0.08 K decade^{-1}) and east Asia (0.09 ± 0.06 K decade^{-1}), as well as Canada (0.10 ± 0.08 K decade^{-1}). DJF warming is largest in similar regions as JJA, including central and north Asia and south Asia (0.17 ± 0.15 and 0.14 ± 0.07 K decade^{-1}) and (although not significant) east Asia (0.12 ± 0.13 K decade^{-1}). Arctic warming is most pronounced during DJF, where the rate of warming is nearly double that during JJA (0.15 ± 0.16 versus 0.08 ± 0.03 K decade^{-1}). As with the annual mean warming, central and north Asia, east Asia, and south Asia generally warm the most during JJA and DJF, with large Arctic warming during DJF.

Regional seasonal precipitation responses continue to exhibit relatively large uncertainty, as most world regions lack a robust response (see also Supplementary Figures 5-6). Central and north Asia, east Asia and south Asia yield robust JJA increases in precipitation under NTCF mitigation. The increase in south and east Asia precipitation is consistent with aerosol reductions driving enhanced monsoonal flow. Interestingly, there is also a large increase in south Asian precipitation during DJF. Canada, south Africa, and north Africa in particular also exhibit robust increases in DJF precipitation. As with the annual mean, most of the increase in DJF precipitation over Africa occurs in east Africa (Supplementary Figure 6).

Seasonal air pollution, including both O_3 and $PM_{2.5}$, also exhibits robust decreases in nearly all world regions. Over land regions, slightly larger O_3 decreases occur during JJA relative to DJF, at $-4.2\pm0.4\%$ decade^{-1} and $-3.2\pm0.8\%$ decade^{-1}, respectively. In contrast, slightly larger $PM_{2.5}$ decreases occur during DJF relative to JJA, at $-7.4\pm1.5\%$ decade^{-1} and $-5.1\pm0.9\%$ decade^{-1}, respectively. As with the annual mean, the largest JJA and DJF O_3 reductions occur over central America and southeast Asia (and south America during DJF). The lone regional increase in O_3 occurs during DJF in east Asia. The largest JJA decreases in $PM_{2.5}$ occur in east Asia, south Asia, and southeast Asia. These regions also exhibit large DJF decreases in $PM_{2.5}$, particularly south Asia at $-26.3\pm5.5\%$ decade^{-1}.

4 Conclusions

Under the experimental protocol of AerChemMIP (Collins et al., 2017), we have analyzed future chemistry-climate simulations to assess the impact of non-methane NTCF mitigation of climate and air quality from 2015-2055. Simulations show robust decreases in air pollution in nearly all world regions. Over global land, surface $PM_{2.5}$ and O_3 decrease by -25% and -16%, respectively, with larger reductions in some world regions including south and southeast Asia. However, NTCF mitigation leads to additional global warming and precipitation increases of 0.23K and 1.2%, respectively. Similar increases in extreme weather indices also occur, including the hottest and wettest day. All world regions yield robust warming in response to NTCF mitigation, with the largest warming (and wetting) occurring over Asia, including central and north Asia, east Asia and south Asia. Relatively large warming also occurs over the Arctic at 0.41K, nearly double the global mean warming.

https://doi.org/10.5194/acp-2019-1209
Preprint. Discussion started: 4 February 2020

Interestingly, models that include both aerosol and ozone reductions (lowAERO3) yield larger warming (and wetting) relative to models that include aerosol reductions alone (lowAER) (0.24 versus 0.20 K, respectively). Although this difference is not significant, it suggests a weak cooling effect due to ozone reductions, or other possible effects from interactive chemistry and aerosol that need to be further explored. For example, aerosol formation may be reduced due to changes in oxidants (from O_3 reductions), which would lead to more surface warming in lowAERO3. Simulations with a single model, running both coupled and uncoupled chemistry experiments, would help isolate this effect.

Our results are consistent with several studies that have shown aerosol reductions will unmask GHG warming, resulting in large, near-tern increases in global warming and precipitation (Brasseur and Roeckner, 2005; Andreae et al., 2005; Ramanathan and Feng, 2008; Raes and Seinfeld, 2009; Kloster et al., 2010; Arneth et al., 2009; Matthews and Zickfeld, 2012; Rotstayn et al., 2013; Wu et al., 2013; Westervelt et al., 2015; Salzmann, 2016; Hienola et al., 2018; Richardson et al., 2018; Samset et al., 2018; Lelieveld et al., 2019). Shindell and Smith (2019), however, show that the time required to transform power generation, industry and transportation leads to largely offsetting climate impacts of CO_2 and sulfur dioxide, implying no conflict between climate and air-quality objectives. There, a 1.5°C mitigation pathway is used, with gradual phasing out of fossil fuel combustion, which leads to relatively small change in the near-future warming. Furthermore, Shindell and Smith (2019) include methane mitigation, which compensates the relatively small near-term future warming from SO_2 reductions.

Our simulations, however, do not account for CO_2 reductions, implying the importance of simultaneous reductions in both CO_2 and NTCFs. We note that it is difficult to reduce only the NTCF emissions while keeping CO_2 emissions fixed (since there are co-emitted species, including SO_2). At the same time, however, the lowNTCF scenario can be used to provide forcing and response sensitivities under current climate, which could be used by intermediate complex models for testing out more scenarios which include complex NTCF-CO_2 reduction scenarios. Furthermore, AerChemMIP simulations do not account for methane reductions, which is another NTCF that, if reduced, will promote cooling. As the strong air quality control pathway includes methane reductions (100% reduction relative to weak air quality control), additional simulations should be conducted that include the effects of all NTCFs, including aerosols, ozone precursor gases and methane. It is likely that inclusion of methane will offset some of the warming reported here, and also impact tropospheric O_3 and air quality. However, simulations with a simple emissions-based climate model show that across the SSPs, methane mitigation cannot fully cancel out the near-term warming from reductions of non-methane NTCFs (P. Zanis 2019, personal communication, December 26th). Although not addressed in this study, we also note the potential role of hydrofluorocarbon (HFC) mitigation through the Kigali Amendment, particularly for the late 21st century. Efficient implementation of the Kigali Amendment and national regulations is estimated to lead to relatively small cooling (<0.07°C) by 2050, but this increases to cooling of 0.2-0.4°C by 2100 (WMO, 2018). Nonetheless, cleaning the air while keeping global warming below the 1.5-2° Paris Agreement climate target will likely require simultaneous cuts in both NTCFs and carbon dioxide.

Data availability. GFDL-ESM4 (Horowitz et al., 2018; John et al., 2018), and other CMIP6 model data can be freely downloaded from the ESGF server.

https://doi.org/10.5194/acp-2019-1209
Preprint. Discussion started: 4 February 2020

Atmospheric Chemistry and Physics Discussions

Author contributions. R.J.A. performed the analysis and wrote the paper. D.N., U.L. and I.T. performed MPI-ESM-1-2-HAM simulations. P.N. and M.M. performed CNRM-ESM2-1 simulations. T.W. and J.Z. performed BCC-ESM1 simulations. N.O. and M.D. performed MRI-ESM2-0 simulations. T.T. performed MIROC6 simulations. L.E. and J-F.L. performed CESM2 and CESM2-WACCM simulations. L.H., V.N. and L.S. performed GFDL-ESM4 simulations. W.J.C., J-F.L. and M.S. originally conceived the AerChemMIP project, including the low NTCF simulations analyzed here. All authors contributed to editing the manuscript.

Competing interests. The authors declare that they have no competing financial interests.

Acknowledgements. T. Takemura was supported by the supercomputer system of the National Institute for Environmental Studies, Japan, and JSPS KAKENHI Grant Number JP19H05669. D. Neubauer acknowledges funding from the European Union's Horizon 2020 research and innovation programme project FORCeS under grant agreement No 821205 and a grant from the Deutsches Klimarechenzentrum (DKRZ) under project ID 1051. I. Tegen acknowledges the DKRZ (Deutsches Klimarechenzenrtrum) for providing computing resources under project ID 1051 (for MPI-ESM1-2-HAM). The CESM project is supported primarily by the National Science Foundation. This material is based upon work supported by the National Center for Atmospheric Research, which is a major facility sponsored by the NSF under Cooperative Agreement No. 1852977. Computing and data storage resources, including the Cheyenne supercomputer (doi:10.5065/D6RX99HX), were provided by the Computational and Information Systems Laboratory (CISL) at NCAR. S. Shim was supported by the Korea Meteorological Administration Research and Development Program "Development and Assessment of IPCC AR6 Climate Change Scenario", grant agreement number 1365003000.

https://doi.org/10.5194/acp-2019-1209
Preprint. Discussion started: 4 February 2020

Atmospheric Chemistry and Physics Discussions

References

Ackerley, D., Booth, B. B. B., Knight, S. H. E., Highwood, E. J., Frame, D. J., Allen, M. R., and Rowell, D. P.: Sensitivity of twentieth-century Sahel rainfall to sulfate aerosol and CO2 forcing, Journal of Climate, 24, 4999–5014, doi: 10.1175/JCLI–D–11–00 019.1, 2011.

Acosta Navarro, J. C., Varma, V., Riipinen, I., Seland, Ø., Kirkevåg, A., Struthers, H., Iversen, T., Hansson, H. C., and Ekman, A. M. L.: Amplification of Arctic warming by past air pollution reductions in Europe, Nature Geoscience, 9, 277–281, doi: 10.1038/ngeo2673, 2016.

Allen, R. J.: A 21st century northward tropical precipitation shift caused by future anthropogenic aerosol reductions, Journal of Geophysical Research: Atmospheres, 120, 9087–9102, doi: 10.1002/2015JD023 623, 2015.

Allen, R. J. and Ajoku, O.: Future aerosol reduction and widening of the nothern tropical belt, J. Geophys. Res., pp. 1–22, doi: 10.1002/2016JD024 803, 2016.

Allen, R. J. and Sherwood, S. C.: The impact of natural versus anthropogenic aerosols on atmospheric circulation in the Community Atmosphere Model, Climate Dyn., 36, 1959–1978, doi: 10.1007/s00 382–010–0898–8, 2011.

Allen, R. J., Evan, A. T., and Booth, B. B. B.: Interhemispheric Aerosol Radiative Forcing and Tropical Precipitation Shifts during the Late Twentieth Century, Journal of Climate, 28, 8219–8246, doi: 10.1175/JCLI–D–15–0148.1, 2015.

Allen, R. J., Landuyt, W., and Rumbold, S. T.: An increase in aerosol burden and radiative effects in a warmer world, Nature Climate Change, 6, 269–274, doi: 10.1038/nclimate2827, 2016.

Allen, R. J., Amiri-Farahani, A., Lamarque, J.-F., Smith, C., Shindell, D., Hassan, T., and Chung, C. E.: Observationally-constrained aerosol-cloud semi-direct effects, npj Climate and Atmospheric Science, 2019a.

Allen, R. J., Hassan, T., Randles, C. A., and Su, H.: Enhanced land-sea warming contrast elevates aerosol pollution in a warmer world, Nature Climate Change, 9, 300–305, doi: 10.1038/s41 558–019–0401–4, 2019b.

Andreae, M. O., Jones, C. D., and Cox, P. M.: Strong present-day aerosol cooling implies a hot future, Nature, 435, 1187–1190, doi: 10.1038/nature03 671, 2005.

Arneth, A., Unger, N., Kulmala, M., and Andreae, M. O.: Clean the Air, Heat the Planet?, Science, 326, 672–673, doi: 10.1126/science.1181 568, 2009.

Ban-Weiss, G. A., Cao, L., Bala, G., and Caldeira, K.: Dependence of climate forcing and response on the altitude of black carbon aerosols, Climate Dyn., 38, 897–911, doi: 10.1007/s00 382–011–1052–y, 2012.

Bellouin, N., Quaas, J., Gryspeerdt, E., Kinne, S., Stier, P., Watson-Parris, D., Boucher, O., Carslaw, K., Christensen, M., Daniau, A.-L., Dufresne, J.-L., Feingold, G., Fiedler, S., Forster, P., Gettelman, A., Haywood, J., Lohmann, U., Malavelle, F., Mauritsen, T., McCoy, D., Myhre, G., Mülmenstädt, J., Neubauer, D., Possner, A., Rugenstein, M., Sato, Y., Schulz, M., Schwartz, S., Sourdeval, O., Storelvmo, T., Toll, V., Winker, D., and Stevens, B.: Bounding global aerosol radiative forcing of climate change, Reviews of Geophysics, p. doi: 10.1029/2019RG000660, in press.

Biasutti, M.: Forced Sahel rainfall trends in the CMIP5 archive, Journal of Geophysical Research: Atmospheres, 118, 1613–1623, doi: 10.1002/jgrd.50 206, 2013.

Biasutti, M. and Giannini, A.: Robust Sahel drying in response to late 20th century forcings, Geophysical Research Letters, 33, doi: 10.1029/2006GL026 067, 2006.

Bond, T. C., Doherty, S. J., Hahey, D. W., and et al.: Bounding the role of black carbon in the climate system: A scientific assessment, J. Geophys. Res., 118, 5380–5552, doi:10.1002/jgrd.50 171, 2013.

https://doi.org/10.5194/acp-2019-1209
Preprint. Discussion started: 4 February 2020

Boucher, O., Randall, D., Artaxo, P., Bretherton, C., Feingold, G., Forster, P., Kerminen, V.-M., Kondo, Y., Liao, H., Lohmann, U., Rasch, P., Satheesh, S., Sherwood, S., Stevens, B., and Zhang, X.: Clouds and Aerosols. In: Climate Change 2013: The Physical Science Basis. Contribution of Working Group I to the Fifth Assessment Report of the Intergovernmental Panel on Climate Change [Stocker, T.F., D. Qin, G.-K. Plattner, M. Tignor, S.K. Allen, J. Boschung, A. Nauels, Y. Xia, V. Bex and P.M. Midgley (eds.)], Tech. rep., Cambridge University Press, Cambridge, United Kingdom and New York, NY, USA, 2013.

Brasseur, G. P. and Roeckner, E.: Impact of improved air quality on the future evolution of climate, Geophysical Research Letters, 32, doi: 10.1029/2005GL023 902, 2005.

Buchard, V., Randles, C. A., da Silva, A. M., Darmenov, A., Colarco, P. R., Govindaraju, R., Ferrare, R., Hair, J., Beyersdorf, A. J., Ziemba, L. D., and Yu, H.: The MERRA-2 Aerosol Reanalysis, 1980 Onward. Part II: Evaluation and Case Studies, Journal of Climate, 30, 6851–6872, doi: 10.1175/JCLI–D–16–0613.1, 2017.

Butt, E. W., Turnock, S. T., Rigby, R., Reddington, C. L., Yoshioka, M., Johnson, J. S., Regayre, L. A., Pringle, K. J., Mann, G. W., and Spracklen, D. V.: Global and regional trends in particulate air pollution and attributable health burden over the past 50 years, Environmental Research Letters, 12, 104 017, doi: 10.1088/1748–9326/aa87be, 2017.

Cai, W., Bi, D., Church, J., Cowan, T., Dix, M., and Rotstayn, L.: Pan-oceanic response to increasing anthropogenic aerosols: Impacts on the Southern Hemisphere oceanic circulation, Geophysical Research Letters, 33, doi: 10.1029/2006GL027 513, 2006.

Chang, C.-Y., Chiang, J. C. H., Wehner, M. F., Friedman, A. R., and Ruedy, R.: Sulfate Aerosol Control of Tropical Atlantic Climate over the Twentieth Century, Journal of Climate, 24, 2540–2555, doi: 10.1175/2010JCLI4065.1, 2011.

Cohen, A. J., Brauer, M., Burnett, R., Anderson, H. R., Frostad, J., Estep, K., Balakrishnan, K., Brunekreef, B., Dandona, L., Dandona, R., Feigin, V., Freedman, G., Hubbell, B., Jobling, A., Kan, H., Knibbs, L., Liu, Y., Martin, R., Morawska, L., Pope, C. A., Shin, H., Straif, K., Shaddick, G., Thomas, M., van Dingenen, R., van Donkelaar, A., Vos, T., Murray, C. J. L., and Forouzanfar, M. H.: Estimates and 25-year trends of the global burden of disease attributable to ambient air pollution: an analysis of data from the Global Burden of Diseases Study 2015, The Lancet, 389, 1907–1918, doi: 10.1016/S0140–6736(17)30 505–6, 2017.

Collins, W. J., Lamarque, J.-F., Schulz, M., Boucher, O., Eyring, V., Hegglin, M. I., Maycock, A., Myhre, G., Prather, M., Shindell, D., and Smith, S. J.: AerChemMIP: quantifying the effects of chemistry and aerosols in CMIP6, Geoscientific Model Development, 10, 585–607, doi: 10.5194/gmd–10–585–2017, 2017.

Delworth, T. L. and Dixon, K. W.: Have anthropogenic aerosols delayed a greenhouse gas-induced weakening of the North Atlantic thermohaline circulation?, Geophysical Research Letters, 33, doi: 10.1029/2005GL024 980, 2006.

Donat, M., Alexander, L., Yang, H., Durre, I., Vose, R., and Caesar, J.: Global Land-Based Datasets for Monitoring Climatic Extremes, Bulletin of the American Meteorological Society, 94, 997–1006, doi: 10.1175/BAMS–D–12–00 109.1, 2013a.

Donat, M. G., Alexander, L. V., Yang, H., Durre, I., Vose, R., Dunn, R. J. H., Willett, K. M., Aguilar, E., Brunet, M., Caesar, J., Hewitson, B., Jack, C., Klein Tank, A. M. G., Kruger, A. C., Marengo, J., Peterson, T. C., Renom, M., Oria Rojas, C., Rusticucci, M., Salinger, J., Elrayah, A. S., Sekele, S. S., Srivastava, A. K., Trewin, B., Villarroel, C., Vincent, L. A., Zhai, P., Zhang, X., and Kitching, S.: Updated analyses of temperature and precipitation extreme indices since the beginning of the twentieth century: The HadEX2 dataset, J. Geophys. Res.-Atmos., 118, 2098–2118, doi: 10.1002/jgrd.50 150, 2013b.

Dong, B., Sutton, R. T., Highwood, E., and Wilcox, L.: The Impacts of European and Asian Anthropogenic Sulfur Dioxide Emissions on Sahel Rainfall, Journal of Climate, 27, 7000–7017, doi: 10.1175/JCLI–D–13–00 769.1, 2014.

Dunne, J. P. and et al.: The GFDL Earth System Model version 4.1 (GFDL-ESM4.1): Model description and simulation characteristics, Journal of Advances in Modeling Earth Systems, In prep.

https://doi.org/10.5194/acp-2019-1209
Preprint. Discussion started: 4 February 2020

Atmospheric Chemistry and Physics Discussions

Emmons, L. K., Orlando, J. J., Tyndall, G., Schwantes, R. H., Kinnison, D., Lamarque, J.-F., Marsh, D., Mills, M., Tilmes, S., Buchholtz, R. R., Gettelman, A., Garcia, R., Simpson, I., Blake, D. R., G., and Pétron: The Chemistry Mechanism in the Community Earth System Model verson 2 (CESM2), J. Adv. Model. Earth Syst., submitted, 2019.

Eyring, V., Bony, S., Meehl, G. A., Senior, C. A., Stevens, B., Stouffer, R. J., and Taylor, K. E.: Overview of the Coupled Model Intercomparison Project Phase 6 (CMIP6) experimental design and organization, Geoscientific Model Development, 9, 1937–1958, doi: 10.5194/gmd–9–1937–2016, 2016.

Fiore, A. M., Naik, V., Spracklen, D. V., Steiner, A., Unger, N., Prather, M., Bergmann, D., Cameron-Smith, P. J., Cionni, I., Collins, W. J., Dalsøren, S., Eyring, V., Folberth, G. A., Ginoux, P., Horowitz, L. W., Josse, B., Lamarque, J.-F., MacKenzie, I. A., Nagashima, T., O'Connor, F. M., Righi, M., Rumbold, S. T., Shindell, D. T., Skeie, R. B., Sudo, K., Szopa, S., Takemura, T., and Zeng, G.: Global air quality and climate, Chem. Soc. Rev., 41, 6663–6683, doi: 10.1039/C2CS35 095E, 2012.

Forster, P. M., Richardson, T., Maycock, A. C., Smith, C. J., Samset, B. H., Myhre, G., Andrews, T., Pincus, R., and Schulz, M.: Recommendations for diagnosing effective radiative forcing from climate models for CMIP6, Journal of Geophysical Research: Atmospheres, 121, 12,460–12,475, doi: 10.1002/2016JD025 320, 2016.

Fujimori, S., Hasegawa, T., Masui, T., Takahashi, K., Herran, D. S., Dai, H., Hijioka, Y., and Kainuma, M.: SSP3: AIM implementation of Shared Socioeconomic Pathways, Global Environmental Change, 42, 268–283, doi: 10.1016/j.gloenvcha.2016.06.009, 2017.

Gettelman, A., Mills, M. J., Kinnison, D. E., Garcia, R. R., Smith, A. K., Marsh, D. R., Tilmes, S., Vitt, F., Bardeen, C. G., McInerny, J., Liu, H.-L., Solomon, S. C., Polvani, L. M., Emmons, L. K., Lamarque, J.-F., Richter, J. H., Glanville, A. S., Bacmeister, J. T., Phillips, A. S., Neale, R. B., Simpson, I. R., DuVivier, A. K., Hodzic, A., and Randel, W. J.: The Whole Atmosphere Community Climate Model Version 6 (WACCM6), Journal of Geophysical Research: Atmospheres, p. doi: 10.1029/2019JD030943, in press.

Gidden, M. J., Riahi, K., Smith, S. J., Fujimori, S., Luderer, G., Kriegler, E., van Vuuren, D. P., van den Berg, M., Feng, L., Klein, D., Calvin, K., Doelman, J. C., Frank, S., Fricko, O., Harmsen, M., Hasegawa, T., Havlik, P., Hilaire, J., Hoesly, R., Horing, J., Popp, A., Stehfest, E., and Takahashi, K.: Global emissions pathways under different socioeconomic scenarios for use in CMIP6: a dataset of harmonized emissions trajectories through the end of the century, Geoscientific Model Development, 12, 1443–1475, doi: 10.5194/gmd–12–1443–2019, 2019.

Guo, L., Turner, A. G., and Highwood, E. J.: Local and Remote Impacts of Aerosol Species on Indian Summer Monsoon Rainfall in a GCM, Journal of Climate, 29, 6937–6955, doi: 10.1175/JCLI–D–15–0728.1, 2016.

Hassan, T., Allen, R. J., Liu, W., and Randles, C.: Aerosol induced weakening of the Atlantic Meridional Overturning Circulation, In prep.

Hienola, A., Partanen, A.-I., Pietikäinen, J.-P., O'Donnell, D., Korhonen, H., Matthews, H. D., and Laaksonen, A.: The impact of aerosol emissions on the 1.5 °C pathways, Environmental Research Letters, 13, 044 011, doi: 10.1088/1748–9326/aab1b2, 2018.

Horowitz, L. W. and et al.: The GFDL Global Atmospheric Chemistry-Climate Model AM4.1: Model Description and Simulation Characteristics, Journal of Advances in Modeling Earth Systems, In prep.

Horowitz, L. W., Naik, V., Sentman, L. T., Paulot, F., Blanton, C., McHugh, C., Radhakrishnan, A., Rand, K., Ginoux, P., and Paynter, D. J.: NOAA-GFDL GFDL-ESM4 model output prepared for CMIP6 AerChemMIP, Version YYYYMMDD[1].Earth System Grid Federation., p. https://doi.org/10.22033/ESGF/CMIP6.1404, 2018.

Hwang, Y.-T., Frierson, D. M. W., and Kang, S. M.: Anthropogenic sulfate aerosol and the southward shift of tropical precipitation in the late 20th century, Geophysical Research Letters, 40, 2845–2850, doi: 10.1002/grl.50 502, 2013.

John, J. G., Blanton, C., McHugh, C., Nikonov, S., Radhakrishnan, A., Rand, K., Vahlenkamp, H., Zadeh, N. T., Gauthier, P., Ginoux, P., Harrison, M., Horowitz, L., Malyshev, S., Naik, V., Paynter, D. J., Ploshay, J., Silvers, L., Stock, C., Winton, M., Zeng, Y., and Dunne, J. P.:

https://doi.org/10.5194/acp-2019-1209
Preprint. Discussion started: 4 February 2020

NOAA-GFDL GFDL-ESM4 model output prepared for CMIP6 ScenarioMIP., Version YYYYMMDD[1].Earth System Grid Federation., p. https://doi.org/10.22033/ESGF/CMIP6.1414, 2018.

Johnson, B. T., Haywood, J. M., and Hawcroft, M. K.: Are Changes in Atmospheric Circulation Important for Black Carbon Aerosol Impacts on Clouds, Precipitation, and Radiation?, Journal of Geophysical Research: Atmospheres, 124, 7930–7950, doi: 10.1029/2019JD030 568, 2019.

Joshi, M. M., Gregory, J. M., Webb, M. J., Sexton, D. M. H., and Johns, T. C.: Mechanisms for the land/sea warming contrast exhibited by simulations of climate change, Climate Dyn., 30, 455–465, doi:10.1007/s00 382–007–0306–1, 2008.

Kloster, S., Dentener, F., Feichter, J., Raes, F., Lohmann, U., Roeckner, E., and Fischer-Bruns, I.: A GCM study of future climate response to aerosol pollution reductions, Climate Dynamics, 34, 1177–1194, doi: 10.1007/s00 382–009–0573–0, 2010.

Krishnan, R., Sabin, T. P., Vellore, R., Mujumdar, M., Sanjay, J., Goswami, B. N., Hourdin, F., Dufresne, J.-L., and Terray, P.: Deciphering the desiccation trend of the South Asian monsoon hydroclimate in a warming world, Climate Dynamics, 47, 1007–1027, doi: 10.1007/s00 382–015–2886–5, 2016.

Lau, W. K.-M. and Kim, K.-M.: Competing influences of greenhouse warming and aerosols on Asian summer monsoon circulation and rainfall, Asia-Pacific Journal of Atmospheric Sciences, 53, 181–194, doi: 10.1007/s13 143–017–0033–4, 2017.

Lelieveld, J., Klingmüller, K., Pozzer, A., Burnett, R. T., Haines, A., and Ramanathan, V.: Effects of fossil fuel and total anthropogenic emission removal on public health and climate, Proceedings of the National Academy of Sciences, 116, 7192–7197, doi: 10.1073/pnas.1819989 116, 2019.

Levy, H., Horowitz, L. W., Schwarzkopf, M. D., Ming, Y., Golaz, J.-C., Naik, V., and Ramaswamy, V.: The roles of aerosol direct and indirect effects in past and future climate change, J. Geophys. Res, 118, 4521–4532, doi: 10.1002/jgrd.50 192, 2013.

Lewinschal, A., Ekman, A. M. L., Hansson, H.-C., Sand, M., Berntsen, T. K., and Langner, J.: Local and remote temperature response of regional SO_2 emissions, Atmospheric Chemistry and Physics, 19, 2385–2403, doi: 10.5194/acp–19–2385–2019, 2019.

Li, X., Ting, M., Li, C., and Henderson, N.: Mechanisms of Asian Summer Monsoon Changes in Response to Anthropogenic Forcing in CMIP5 Models, Journal of Climate, 28, 4107–4125, doi: 10.1175/JCLI–D–14–00 559.1, 2015.

Liepert, B. G., Feichter, J., Lohmann, U., and Roeckner, E.: Can aerosols spin down the water cycle in a warmer and moister world?, Geophys. Res. Lett., 31, L06 207, doi: 10.1029/2003GL019 060, 2004.

Lin, L., Xu, Y., Wang, Z., Diao, C., Dong, W., and Xie, S.-P.: Changes in Extreme Rainfall Over India and China Attributed to Regional Aerosol-Cloud Interaction During the Late 20th Century Rapid Industrialization, Geophysical Research Letters, 45, 7857–7865, doi: 10.1029/2018GL078 308, 2018.

Liu, L., Shawki, D., Voulgarakis, A., Kasoar, M., Samset, B. H., Myhre, G., Forster, P. M., Hodnebrog, Ø., Sillmann, J., Aalbergsjø, S. G., Boucher, O., Faluvegi, G., Iversen, T., Kirkevåg, A., Lamarque, J.-F., Olivié, D., Richardson, T., Shindell, D., and Takemura, T.: A PDRMIP Multimodel Study on the Impacts of Regional Aerosol Forcings on Global and Regional Precipitation, Journal of Climate, 31, 4429–4447, doi: 10.1175/JCLI–D–17–0439.1, 2018.

Matthews, H. D. and Zickfeld, K.: Climate response to zeroed emissions of greenhouse gases and aerosols, Nature Climate Change, 2, 338–341, doi: 10.1038/nclimate1424, 2012.

Mauritsen, T., Bader, J., Becker, T., Behrens, J., Bittner, M., Brokopf, R., Brovkin, V., Claussen, M., Crueger, T., Esch, M., Fast, I., Fiedler, S., Fläschner, D., Gayler, V., Giorgetta, M., Goll, D. S., Haak, H., Hagemann, S., Hedemann, C., Hohenegger, C., Ilyina, T., Jahns, T., Jimenéz-de-la Cuesta, D., Jungclaus, J., Kleinen, T., Kloster, S., Kracher, D., Kinne, S., Kleberg, D., Lasslop, G., Kornblueh, L., Marotzke, J., Matei, D., Meraner, K., Mikolajewicz, U., Modali, K., Möbis, B., Müller, W. A., Nabel, J. E. M. S., Nam, C. C. W., Notz,

https://doi.org/10.5194/acp-2019-1209
Preprint. Discussion started: 4 February 2020

D., Nyawira, S.-S., Paulsen, H., Peters, K., Pincus, R., Pohlmann, H., Pongratz, J., Popp, M., Raddatz, T. J., Rast, S., Redler, R., Reick, C. H., Rohrschneider, T., Schemann, V., Schmidt, H., Schnur, R., Schulzweida, U., Six, K. D., Stein, L., Stemmler, I., Stevens, B., von Storch, J.-S., Tian, F., Voigt, A., Vrese, P., Wieners, K.-H., Wilkenskjeld, S., Winkler, A., and Roeckner, E.: Developments in the MPI-M Earth System Model version 1.2 (MPI-ESM1.2) and Its Response to Increasing CO2, Journal of Advances in Modeling Earth Systems, 11, 998–1038, doi: 10.1029/2018MS001 400, 2019.

Menary, M. B., Roberts, C. D., Palmer, M. D., Halloran, P. R., Jackson, L., Wood, R. A., Müller, W. A., Matei, D., and Lee, S.-K.: Mechanisms of aerosol-forced AMOC variability in a state of the art climate model, Journal of Geophysical Research: Oceans, 118, 2087–2096, doi: 10.1002/jgrc.20 178, 2013.

Michou, M., Nabat, P., Saint-Martin, D., Bock, J., Decharme, B., Mallet, M., Roehrig, R., Séférian, R., Sénési, S., and Voldoire, A.: Present-day and historical aerosol and ozone characteristics in CNRM CMIP6 simulations, Journal of Advances in Modeling Earth Systems, p. doi: 10.1029/2019MS001816, 2019.

Ming, Y., Ramaswamy, V., and Persad, G.: Two opposing effects of absorbing aerosols on global-mean precipitation, Geophys. Res. Lett., 37, L13 701, doi: 10.1029/2010GL042 895, 2010.

Myhre, G., Shindell, D., Bréon, F.-M., Collins, W., Fuglestvedt, J., Huang, J., Koch, D., Lamarque, J.-F., Lee, D., Mendoza, B., Nakajima, T., Robock, A., Stephens, G., Takemura, T., and Zhang, H.: Anthropogenic and Natural Radiative Forcing. In: Climate Change 2013: The Physical Science Basis. Contribution of Working Group I to the Fifth Assessment Report of the Intergovernmental Panel on Climate Change [Stocker, T.F., D. Qin, G.-K. Plattner, M. Tignor, S.K. Allen, J. Boschung, A. Nauels, Y. Xia, V. Bex and P.M. Midgley (eds.)], Tech. rep., Cambridge University Press, Cambridge, United Kingdom and New York, NY, USA, 2013.

Neubauer, D., Ferrachat, S., Siegenthaler-Le Drian, C., Stier, P., Partridge, D. G., Tegen, I., Bey, I., Stanelle, T., Kokkola, H., and Lohmann, U.: The global aerosol–climate model ECHAM6.3–HAM2.3 – Part 2: Cloud evaluation, aerosol radiative forcing, and climate sensitivity, Geoscientific Model Development, 12, 3609–3639, doi: 10.5194/gmd–12–3609–2019, 2019.

O'Neill, B. C., Kriegler, E., Riahi, K., Ebi, K. L., Hallegatte, S., Carter, T. R., Mathur, R., and van Vuuren, D. P.: A new scenario framework for climate change research: the concept of shared socioeconomic pathways, Climatic Change, 122, 387–400, doi: 10.1007/s10 584–013–0905–2, 2014.

Pincus, R., Forster, P. M., and Stevens, B.: The Radiative Forcing Model Intercomparison Project (RFMIP): experimental protocol for CMIP6, Geoscientific Model Development, 9, 3447–3460, doi: 10.5194/gmd–9–3447–2016, 2016.

Raes, F. and Seinfeld, J. H.: New Directions: Climate change and air pollution abatement: A bumpy road, Atmospheric Environment, 43, 5132 – 5133, doi: 10.1016/j.atmosenv.2009.06.001, 2009.

Ramanathan, V. and Feng, Y.: On avoiding dangerous anthropogenic interference with the climate system: Formidable challenges ahead, Proceedings of the National Academy of Sciences, 105, 14 245–14 250, doi: 10.1073/pnas.0803838 105, 2008.

Ramanathan, V., Crutzen, P. J., Lelieveld, J., Mitra, A. P., and et al.: Indian Ocean Experiment: An integrated analysis of the climate forcing and effects of the great Indo-Asian haze, J. Geophys. Res., 106, 28,371–28,398, 2001.

Randles, C. A., da Silva, A. M., Buchard, V., Colarco, P. R., Darmenov, A., Govindaraju, R., Smirnov, A., Holben, B., Ferrare, R., Hair, J., Shinozuka, Y., and Flynn, C. J.: The MERRA-2 Aerosol Reanalysis, 1980 Onward. Part I: System Description and Data Assimilation Evaluation, Journal of Climate, 30, 6823–6850, doi: 10.1175/JCLI–D–16–0609.1, 2017.

Rao, S., Klimont, Z., Smith, S. J., Dingenen, R. V., Dentener, F., Bouwman, L., Riahi, K., Amann, M., Bodirsky, B. L., van Vuuren, D. P., Reis, L. A., Calvin, K., Drouet, L., Fricko, O., Fujimori, S., Gernaat, D., Havlik, P., Harmsen, M., Hasegawa, T., Heyes, C., Hilaire, J.,

https://doi.org/10.5194/acp-2019-1209
Preprint. Discussion started: 4 February 2020

Luderer, G., Masui, T., Stehfest, E., Strefler, J., van der Sluis, S., and Tavoni, M.: Future air pollution in the Shared Socio-economic Pathways, Global Environmental Change, 42, 346–358, doi: 10.1016/j.gloenvcha.2016.05.012, 2017.

Reddington, C. L., Carslaw, K. S., Stier, P., Schutgens, N., Coe, H., Liu, D., Allan, J., Browse, J., Pringle, K. J., Lee, L. A., Yoshioka, M., Johnson, J. S., Regayre, L. A., Spracklen, D. V., Mann, G. W., Clarke, A., Hermann, M., Henning, S., Wex, H., Kristensen, T. B., Leaitch, W. R., Pöschl, U., Rose, D., Andreae, M. O., Schmale, J., Kondo, Y., Oshima, N., Schwarz, J. P., Nenes, A., Anderson, B., Roberts, G. C., Snider, J. R., Leck, C., Quinn, P. K., Chi, X., Ding, A., Jimenez, J. L., and Zhang, Q.: The Global Aerosol Synthesis and Science Project (GASSP): Measurements and Modeling to Reduce Uncertainty, Bulletin of the American Meteorological Society, 98, 1857–1877, doi: 10.1175/BAMS–D–15–00 317.1, 2017.

Richardson, T. B., Forster, P. M., Andrews, T., Boucher, O., Faluvegi, G., Fläschner, D., Hodnebrog, Ø., Kasoar, M., Kirkevåg, A., Lamarque, J.-F., Myhre, G., Olivié, D., Samset, B. H., Shawki, D., Shindell, D., Takemura, T., and Voulgarakis, A.: Drivers of precipitation change: An energetic understanding, Journal of Climate, 31, 9641–9657, doi: 10.1175/JCLI–D–17–0240.1, 2018.

Rotstayn, L. D. and Lohmann, U.: Tropical rainfall trends and the indirect aerosol effect, J. Climate, 15, 2103–2116, 2002.

Rotstayn, L. D., Collier, M. A., Chrastansky, A., Jeffrey, S. J., and Luo, J. J.: Projected effects of declining aerosol in RCP4.5: unmasking global warming?, Atmos. Chem. Phys., 13, 10 883–10 905, 2013.

Rotstayn, L. D., Collier, M. A., and Luo, J.-J.: Effects of declining aerosols on projections of zonally averaged tropical precipitation, Environmental Research Letters, 10, 044 018, doi: 10.1088/1748–9326/10/4/044 018, 2015.

Salzmann, M.: Global warming without global mean precipitation increase?, Science Advances, 2, doi: 10.1126/sciadv.1501 572, 2016.

Samset, B. H., Myhre, G., Forster, P. M., Hodnebrog, Ø., Andrews, T., Faluvegi, G., Fläschner, D., Kasoar, M., Kharin, V., Kirkevåg, A., Lamarque, J.-F., Olivié, D., Richardson, T., Shindell, D., Shine, K. P., Takemura, T., and Voulgarakis, A.: Fast and slow precipitation responses to individual climate forcers: A PDRMIP multimodel study, Geophysical Research Letters, 43, 2782–2791, 10.1002/2016GL068 064, 2016.

Samset, B. H., Sand, M., Smith, C. J., Bauer, S. E., Forster, P. M., Fuglestvedt, J. S., Osprey, S., and Schleussner, C.-F.: Climate Impacts From a Removal of Anthropogenic Aerosol Emissions, Geophysical Research Letters, 45, 1020–1029, doi: 10.1002/2017GL076 079, 2018.

Scannell, C., Booth, B. B. B., Dunstone, N. J., Rowell, D. P., Bernie, D. J., Kasoar, M., Voulgarakis, A., Wilcox, L. J., Navarro, J. C. A., Seland, Ø., and Paynter, D. J.: The Influence of remote anthropogenic aerosols on future East and West African rainfall,, Journal of Climate, submitted.

Schultz, M., Schröder, S., Lyapina, O., Cooper, O., Galbally, I., Petropavlovskikh, I., von Schneidemesser, E., Tanimoto, H., and et al.: Tropospheric Ozone Assessment Report: Database and Metrics Data of Global Surface Ozone Observations, Elem. Sci. Anth., 5, p. 58, doi: 10.1525/elementa.244, 2017.

Séférian, R., Nabat, P., Michou, M., Saint-Martin, D., Voldoire, A., Colin, J., Decharme, B., Delire, C., Berthet, S., Chevallier, M., Sénési, S., Franchisteguy, L., Vial, J., Mallet, M., Joetzjer, E., Geoffroy, O., Guérémy, J.-F., Moine, M.-P., Msadek, R., Ribes, A., Rocher, M., Roehrig, R., Salas-y Mélia, D., Sanchez, E., Terray, L., Valcke, S., Waldman, R., Aumont, O., Bopp, L., Deshayes, J., Éthé, C., and Madec, G.: Evaluation of CNRM Earth System Model, CNRM-ESM2-1: Role of Earth System Processes in Present-Day and Future Climate, Journal of Advances in Modeling Earth Systems, p. doi: 10.1029/2019MS001791, 2019.

Seneviratne, S., Nicholls, N., Easterling, D., Goodess, C., Kanae, S., Kossin, J., Luo, Y., Marengo, J., McInnes, K., Rahimi, M., Reichstein, M., Sorteberg, A., Vera, C., and Zhang, X.: Changes in climate extremes and their impacts on the natural physical environment. In: Managing the Risks of Extreme Events and Disasters to Advance Climate Change Adaptation, Cambridge University Press, 2012.

https://doi.org/10.5194/acp-2019-1209
Preprint. Discussion started: 4 February 2020

Shindell, D. and Smith, C. J.: Climate and air-quality benefits of a realistic phase-out of fossil fuels, Nature, 573, 408–411, doi: 10.1038/s41 586–019–1554–z, 2019.

Silva, R. A., West, J. J., Lamarque, J.-F., Shindell, D. T., Collins, W. J., Faluvegi, G., Folberth, G. A., Horowitz, L. W., Nagashima, T., Naik, V., Rumbold, S. T., Sudo, K., Takemura, T., Bergmann, D., Cameron-Smith, P., Doherty, R. M., Josse, B., MacKenzie, I. A., Stevenson, D. S., and Zeng, G.: Future global mortality from changes in air pollution attributable to climate change, Nature Climate Change, 7, 647–651, doi: 10.1038/nclimate3354, 2017.

Smith, C. J., Forster, P. M., Allen, M., Leach, N., Millar, R. J., Passerello, G. A., and Regayre, L. A.: FAIR v1.3: a simple emissions-based impulse response and carbon cycle model, Geoscientific Model Development, 11, 2273–2297, doi: 10.5194/gmd–11–2273–2018, 2018.

Song, F., Zhou, T., and Qian, Y.: Responses of East Asian summer monsoon to natural and anthropogenic forcings in the 17 latest CMIP5 models, Geophysical Research Letters, 41, 596–603, doi: 10.1002/2013GL058 705, 2014.

Stjern, C. W., Samset, B. H., Myhre, G., Forster, P. M., Hodnebrog, Ø., Andrews, T., Boucher, O., Faluvegi, G., Iversen, T., Kasoar, M., Kharin, V., Kirkevåg, A., Lamarque, J.-F., Olivié, D., Richardson, T., Shawki, D., Shindell, D., Smith, C. J., Takemura, T., and Voulgarakis, A.: Rapid Adjustments Cause Weak Surface Temperature Response to Increased Black Carbon Concentrations, Journal of Geophysical Research: Atmospheres, 122, 11,462–11,481, doi: 10.1002/2017JD027 326, 2017.

Sutton, R. T., Dong, B., and Gregory, J. M.: Land/sea warming ratio in response to climate change: IPCC AR4 model results and comparison with observations, Geophys. Res. Lett., 34, L02 701, doi:10.1029/2006GL028 164, 2007.

Takemura, T., Nozawa, T., Emori, S., Nakajima, T. Y., and Nakajima, T.: Simulation of climate response to aerosol direct and indirect effects with aerosol transport-radiation model, Journal of Geophysical Research: Atmospheres, 110, doi: 10.1029/2004JD005 029, 2005.

Takemura, T., Egashira, M., Matsuzawa, K., Ichijo, H., O'ishi, R., and Abe-Ouchi, A.: A simulation of the global distribution and radiative forcing of soil dust aerosols at the Last Glacial Maximum, Atmospheric Chemistry and Physics, 9, 3061–3073, doi: 10.5194/acp–9–3061–2009, 2009.

Tatebe, H., Ogura, T., Nitta, T., Komuro, Y., Ogochi, K., Takemura, T., Sudo, K., Sekiguchi, M., Abe, M., Saito, F., Chikira, M., Watanabe, S., Mori, M., Hirota, N., Kawatani, Y., Mochizuki, T., Yoshimura, K., Takata, K., O'ishi, R., Yamazaki, D., Suzuki, T., Kurogi, M., Kataoka, T., Watanabe, M., and Kimoto, M.: Description and basic evaluation of simulated mean state, internal variability, and climate sensitivity in MIROC6, Geoscientific Model Development, 12, 2727–2765, doi: 10.5194/gmd–12–2727–2019, 2019.

Tegen, I., Neubauer, D., Ferrachat, S., Siegenthaler-Le Drian, C., Bey, I., Schutgens, N., Stier, P., Watson-Parris, D., Stanelle, T., Schmidt, H., Rast, S., Kokkola, H., Schultz, M., Schroeder, S., Daskalakis, N., Barthel, S., Heinold, B., and Lohmann, U.: The global aerosol–climate model ECHAM6.3–HAM2.3 – Part 1: Aerosol evaluation, Geoscientific Model Development, 12, 1643–1677, doi: 10.5194/gmd–12–1643–2019, 2019.

Tilmes, S., Hodzic, A., Emmons, L. K., Mills, M. J., Gettelman, A., Kinnison, D. E., Park, M., Lamarque, J.-F., Vitt, F., Shrivastava, M., Campuzano-Jost, P., Jimenez, J. L., and Liu, X.: Climate Forcing and Trends of Organic Aerosols in the Community Earth System Model (CESM2), Journal of Advances in Modeling Earth Systems, p. doi: 10.1029/2019MS001827, in press.

Turnock, S. T., Smith, S., and O'Connor, F. M.: The impact of climate mitigation measures on near term climate forcers, Environmental Research Letters, 14, 104 013, doi: 10.1088/1748–9326/ab4222, 2019a.

Turnock, S. T., Wild, O., Sellar, A., and O'Connor, F. M.: 300 years of tropospheric ozone changes using CMIP6 scenarios with a parameterised approach, Atmospheric Environment, 213, 686–698, doi: 10.1016/j.atmosenv.2019.07.001, 2019b.

https://doi.org/10.5194/acp-2019-1209
Preprint. Discussion started: 4 February 2020

Turnock, S. T., Allen, R. J., Andrews, M., Bauer, S., Emmons, L., Good, P., Horowitz, L., Nabat, P., Naik, V., Neubauer, D., O'Connor, F., Olivie, D., Schultz, M., Sellar, A., Takemura, T., Tilmes, S., Tsigaridis, K., Wu, T., and Zhang, J.: Historical and future changes in air pollutants from CMIP6 models, Atmospheric Chemistry and Physics, submitted.

Undorf, S., Polson, D., Bollasina, M. A., Ming, Y., Schurer, A., and Hegerl, G. C.: Detectable Impact of Local and Remote Anthropogenic Aerosols on the 20th Century Changes of West African and South Asian Monsoon Precipitation, Journal of Geophysical Research: Atmospheres, 123, 4871–4889, doi: 10.1029/2017JD027 711, 2018.

van Vuuren, D. P., Kriegler, E., O'Neill, B. C., Ebi, K. L., Riahi, K., Carter, T. R., Edmonds, J., Hallegatte, S., Kram, T., Mathur, R., and Winkler, H.: A new scenario framework for Climate Change Research: scenario matrix architecture, Climatic Change, 122, 373–386, doi: 10.1007/s10 584–013–0906–1, 2014.

Wang, T., Wang, H. J., Otterå, O. H., Gao, Y. Q., Suo, L. L., Furevik, T., and Yu, L.: Anthropogenic agent implicated as a prime driver of shift in precipitation in eastern China in the late 1970s, Atmospheric Chemistry and Physics, 13, 12 433–12 450, doi: 10.5194/acp–13–12 433–2013, 2013.

Westervelt, D. M., Horowitz, L. W., Naik, V., Golaz, J.-C., and Mauzerall, D. L.: Radiative forcing and climate response to projected 21st century aerosol decreases, Atmospheric Chemistry and Physics, 15, 12 681–12 703, doi: 10.5194/acp–15–12 681–2015, 2015.

Westervelt, D. M., Conley, A. J., Fiore, A. M., Lamarque, J.-F., Shindell, D., Previdi, M., Faluvegi, G., Correa, G., and Horowitz, L. W.: Multimodel precipitation responses to removal of U.S. sulfur dioxide emissions, Journal of Geophysical Research: Atmospheres, 122, 5024–5038, doi: 10.1002/2017JD026 756, 2017.

Westervelt, D. M., Conley, A. J., Fiore, A. M., Lamarque, J.-F., Shindell, D. T., Previdi, M., Mascioli, N. R., Faluvegi, G., Correa, G., and Horowitz, L. W.: Connecting regional aerosol emissions reductions to local and remote precipitation responses, Atmospheric Chemistry and Physics, 18, 12 461–12 475, doi: 10.5194/acp–18–12 461–2018, 2018.

Westervelt, D. M., Mascioli, N. R., Fiore, A. M., Conley, A. J., Lamarque, J.-F., Shindell, D. T., Faluvegi, G., Previdi, M., Correa, G., and Horowitz, L. W.: Local and remote mean and extreme temperature response to regional aerosol emissions reductions, Atmospheric Chemistry and Physics Discussions, 2019, 1–33, doi: 10.5194/acp–2019–1096, 2019.

WHO: Ambient air pollution: A global assessment of exposure and burden of disease, Tech. Rep. ISBN: 9789241511353, World Health Organization, 2016.

Wilcox, L. J., Highwood, E. J., and Dunstone, N. J.: The influence of anthropogenic aerosol on multi-decadal variations of historical global climate, Environ. Res. Lett., 8, doi:10.1088/1748–9326/8/2/024 033, 2013.

WMO: Scientific Assessment of Ozone Depletion: 2018, Tech. Rep. Global Ozone Research and Monitoring Project–Report No. 58, 588 pp., Geneva, Switzerland., World Meteorological Organization, 2018.

Wu, P., Christidis, N., and Stott, P.: Anthropogenic impact on Earth's hydrological cycle, Nature Climate Change, 3, 807 EP –, doi: 10.1038/nclimate1932, 2013.

Wu, T., Lu, Y., Fang, Y., Xin, X., Li, L., Li, W., Jie, W., Zhang, J., Liu, Y., Zhang, L., Zhang, F., Zhang, Y., Wu, F., Li, J., Chu, M., Wang, Z., Shi, X., Liu, X., Wei, M., Huang, A., Zhang, Y., and Liu, X.: The Beijing Climate Center Climate System Model (BCC-CSM): the main progress from CMIP5 to CMIP6, Geoscientific Model Development, 12, 1573–1600, doi: 10.5194/gmd–12–1573–2019, 2019.

Wu, T., Zhang, F., Zhang, J., Jie, W., Zhang, Y., Wu, F., Li, L., Liu, X., Lu, X., Zhang, L., Wang, J., and Hu, A.: Beijing Climate Center Earth System Model version 1 (BCC-ESM1): Model Description and Evaluation, Geoscientific Model Development Discussions, pp. 1–47, doi: 10.5194/gmd–2019–172, submitted.

https://doi.org/10.5194/acp-2019-1209
Preprint. Discussion started: 4 February 2020

Xie, X., Wang, H., Liu, X., Li, J., Wang, Z., and Liu, Y.: Distinct effects of anthropogenic aerosols on the East Asian summer monsoon between multidecadal strong and weak monsoon stages, Journal of Geophysical Research: Atmospheres, 121, 7026–7040, doi: 10.1002/2015JD024 228, 2016.

Yukimoto, S., Kawai, H., Koshiro, T., Oshima, N., Yoshida, K., Urakawa, S., Tsujino, H., Deushi, M., Tanaka, T., Hosaka, M., Yabu, S., Yoshimura, H., Shindo, E., Mizuta, R., Obata, A., Adachi, Y., and Ishii, M.: The Meteorological Research Institute Earth System Model Version 2.0, MRI-ESM2.0: Description and Basic Evaluation of the Physical Component, J. Meteor. Soc. Japan, 97, 931–965, doi: 10.2151/jmsj.2019–051, 2019.

Zanis, P., Akritidis, D., Georgoulias, A. K., Allen, R. J., Bauer, S. E., Cole, J., Johnson, B., Deushi, M., Michou, M., Mulcahy, J., Nabat, P., Olivie, D., Oshima, N., Sima, A., Schulz, M., and Takemura, T.: Fast responses on pre-industrial climate from present-day aerosols in a CMIP6 multi-model study, Atmospheric Chemistry and Physics Discussions, submitted.

Zhang, L., Wu, P., and Zhou, T.: Aerosol forcing of extreme summer drought over North China, Environmental Research Letters, 12, 034 020, doi: 10.1088/1748–9326/aa5fb3, 2017.

Zhao, A. D., Stevenson, D. S., and Bollasina, M. A.: The role of anthropogenic aerosols in future precipitation extremes over the Asian Monsoon Region, Climate Dynamics, 52, 6257–6278, doi: 10.1007/s00 382–018–4514–7, 2018.

https://doi.org/10.5194/acp-2019-1209
Preprint. Discussion started: 4 February 2020

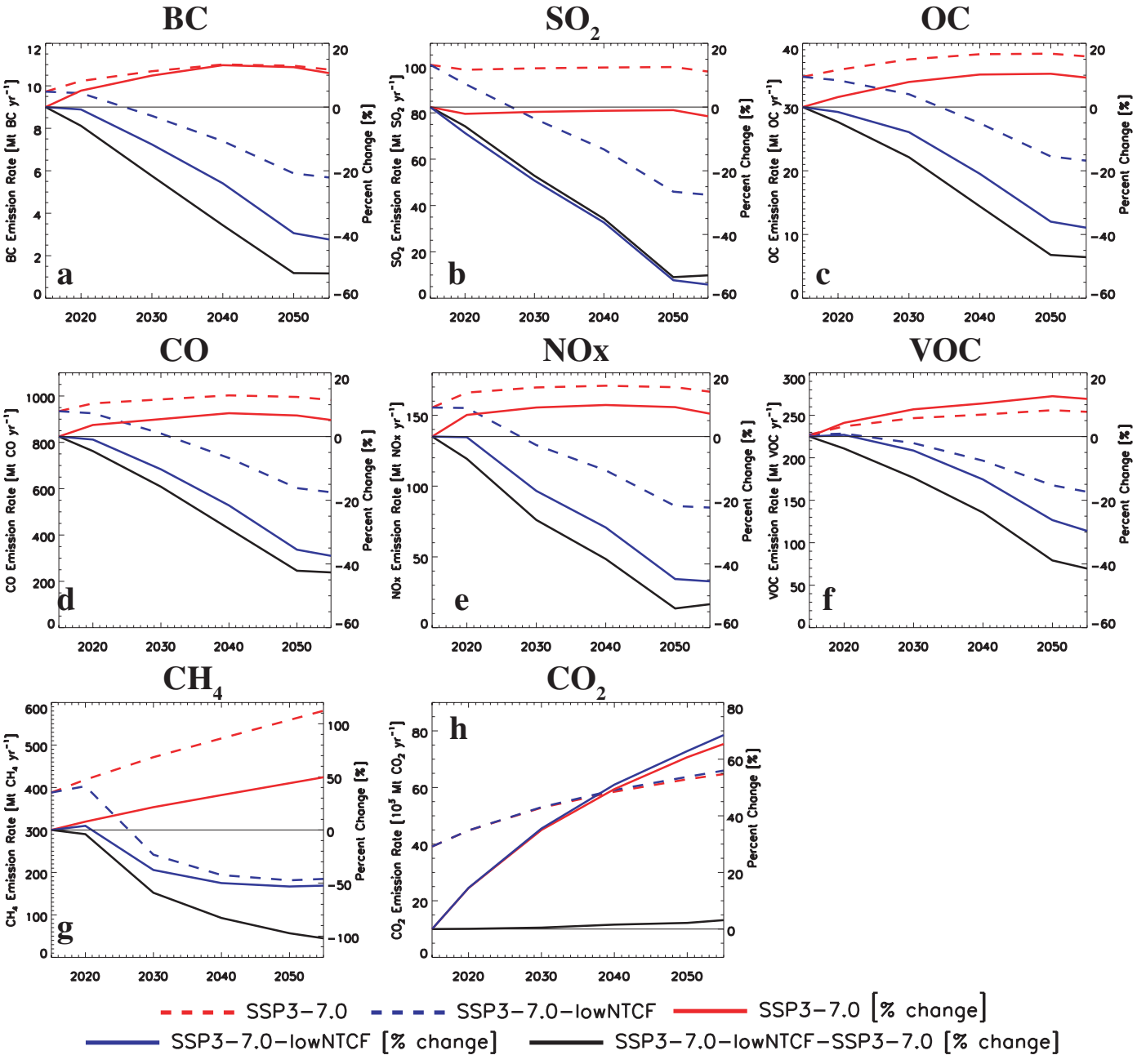

Figure 1. 2015-2055 global mean CO_2, NTCF and precursor gas emissions. Panels show (a) black carbon (BC); (b) sulfur dioxide (SO_2); (c) organic carbon (OC); (d) carbon monoxide (CO); (e) nitrogen oxides (NO_x); (f) volatile organic compounds (VOC); (g) methane (CH_4); and (h) carbon dioxide (CO_2) emissions for weak (SSP3-7.0; red) and strong (SSP3-7.0-lowNTCF; blue) air quality control. Also included is the percent change (relative to 2015) for SSP3-7.0 (red solid), SSP3-7.0-lowNTCF (blue solid), and the difference between the two scenarios (NTCF mitigation; SSP3-7.0-lowNTCF−SSP3-7.0; black solid). Emission units for species X are Mt X yr^{-1}. Percent change units are %. We reiterate that AerChemMIP simulations include the same change in methane emissions, which follow SSP3-7.0.

https://doi.org/10.5194/acp-2019-1209
Preprint. Discussion started: 4 February 2020

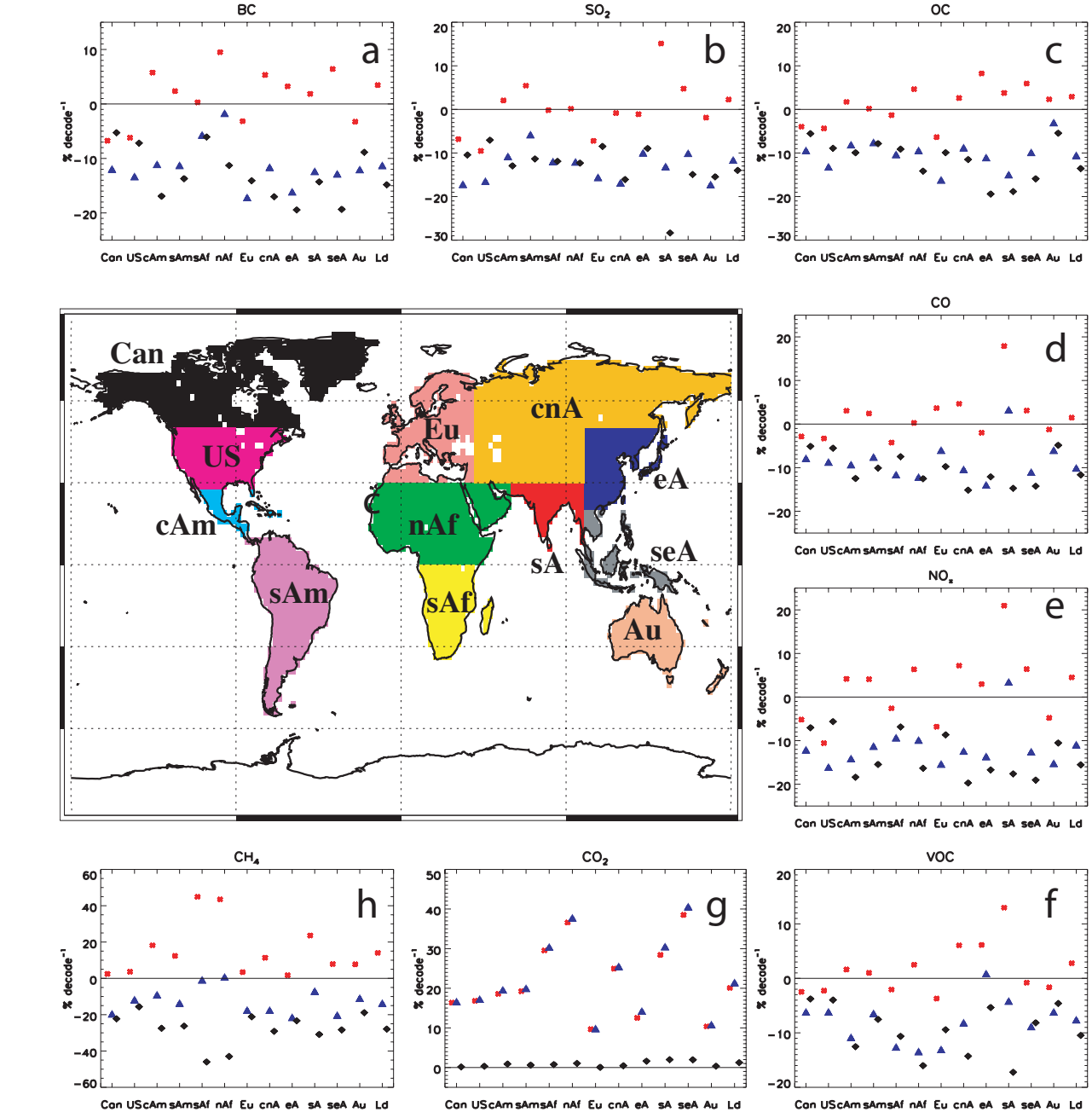

Figure 2. 2015-2055 regional mean CO_2, NTCF and precursor gas emission trends. Regional 2015-2055 emission trends for (a) black carbon (BC); (b) sulfur dioxide (SO_2); (c) organic carbon (OC); (d) carbon monoxide (CO); (e) nitrogen oxides (NO_x); (f) volatile organic compounds (VOC); (g) methane (CH_4); and (h) carbon dioxide (CO_2) for weak (SSP3-7.0; red astrisks) and strong air quality control (SSP3-7.0-lowNTCF; blue triangles) and the difference between the two scenarios (NTCF mitigation; SSP3-7.0-lowNTCF−SSP3-7.0; black diamonds). Center map shows the corresponding color coded world regions, based on Seneviratne et al. (2012). The following abbreviations are used: Canada (Can; black), United States (US; magenta), central America (cAm; sky blue), south America (sAm; purple), south Africa (sAf; yellow), north Africa (nAf; green), Europe (Eu; pink), central and north Asia (cnA; orange), east Asia (eA; navy), south Asia (sA; red), southeast Asia (seA; gray), and Australia (Au; beige). The average over these 12 land regions is abbreviated as "Ld". Trend units are % decade^{-1} (relative to 2015). Note that AerChemMIP simulations include the same change in methane emissions, based on SSP3-7.0.

https://doi.org/10.5194/acp-2019-1209
Preprint. Discussion started: 4 February 2020

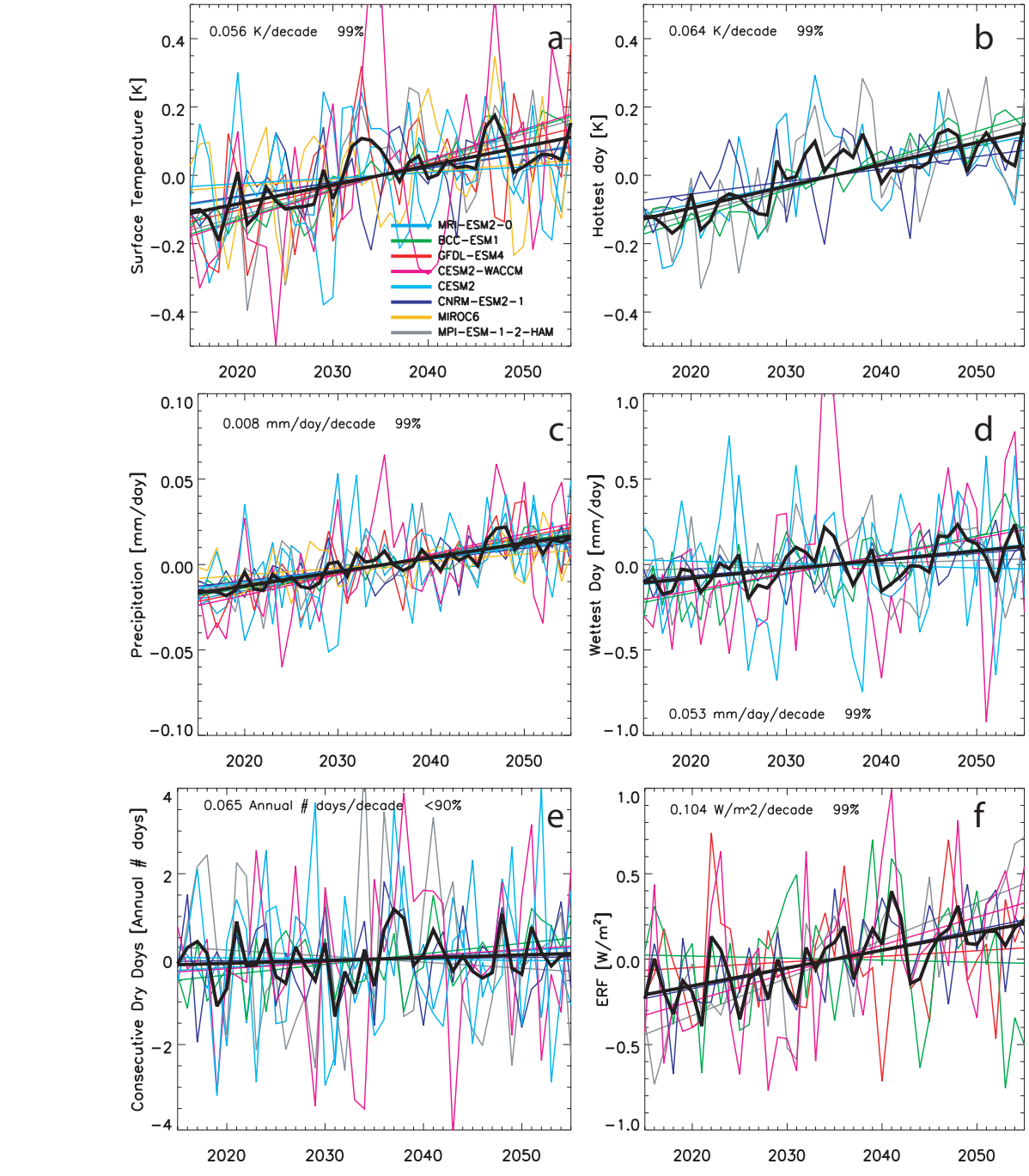

Figure 3. 2015-2055 time series of global annual mean climate anomalies due to NTCF mitigation Panels show (a) surface temperature [K]; (b) hottest day [K]; (c) precipitation [mm day^{-1}]; (d) wettest day [mm day^{-1}]; (e) consecutive dry days [annual number of days]; and (f) effective radiative forcing (ERF) [W m^{-2}] for the difference between the two scenarios (NTCF mitigation; SSP3-7.0-lowNTCF−SSP3-7.0). Anomalies are relative to the global annual mean 2015-2055 climatology. The ensemble mean time series, and the corresponding trend, are included as thick black lines. The ensemble mean trend and its significance are also included.

https://doi.org/10.5194/acp-2019-1209
Preprint. Discussion started: 4 February 2020

Atmospheric Chemistry and Physics Discussions

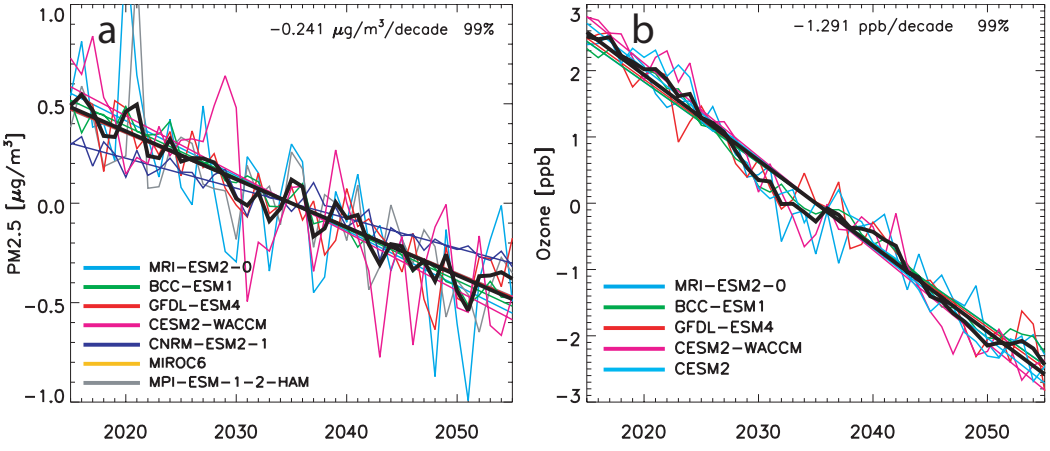

Figure 4. 2015-2055 time series of global annual mean air pollution anomalies due to NTCF mitigation Panels show (a) surface particulate matter ($PM_{2.5}$) [μg m^{-3}] and (b) surface ozone [ppb] for the difference between the two scenarios (NTCF mitigation; SSP3-7.0-lowNTCF−SSP3-7.0). Anomalies are relative to the global annual mean 2015-2055 climatology. The ensemble mean time series, and the corresponding trend, are included as thick black lines. The ensemble mean trend and its significance are also included.

https://doi.org/10.5194/acp-2019-1209
Preprint. Discussion started: 4 February 2020

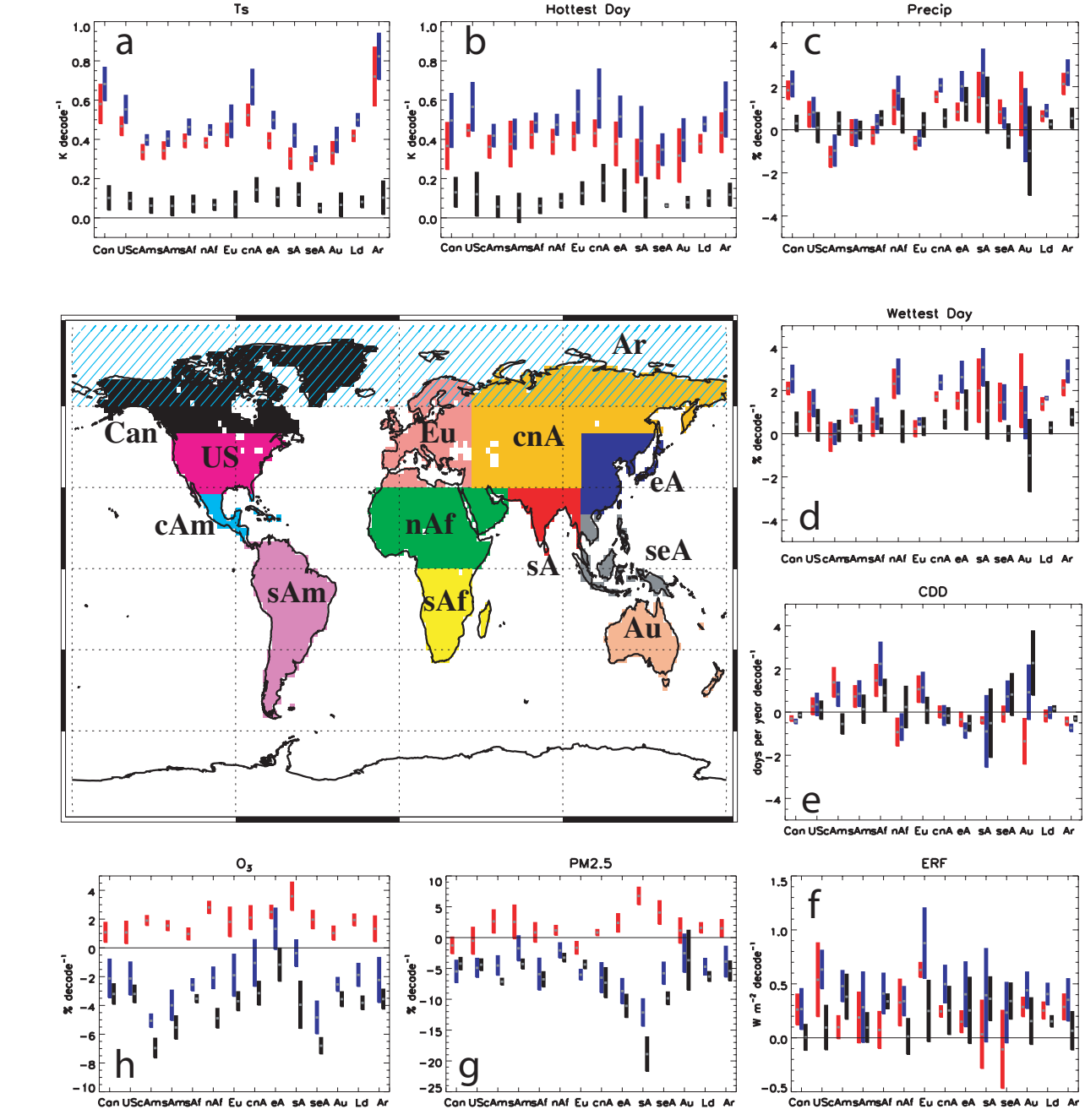

Figure 5. Regional climate and air pollution responses to NTCF mitigation. Bar plots show regional 2015-2055 trends in (a) surface temperature (T_s); (b) hottest day; (c) precipitation (Precip); (d) wettest day; (e) consecutive dry days (CDD); (f) effective radiative forcing (ERF); (g) surface particulate matter ($PM_{2.5}$) and (h) ozone (O_3) for weak (SSP3-7.0; red) and strong (SSP3-7.0-lowNTCF; blue) air quality control, and the difference between the two scenarios (NTCF mitigation; SSP3-7.0-lowNTCF−SSP3-7.0; black). Bar center (gray horizontal line) shows the multimodel mean. Bar length represents the trend uncertainty, estimated as $2\sigma/\sqrt{n}$, where σ is the standard deviation of the trends and n is the number of models. Center map shows the corresponding color coded world regions for each bar plot (as in Fig. 2). The average over these 12 land regions is abbreviated as "Ld". Also included is the Arctic ("Ar"), defined as poleward of 60N (light blue hatched region). Trend units are K decade^{-1} for T_s and hottest day; % decade^{-1} for Precip, wettest day, $PM_{2.5}$ and O_3; days per year decade^{-1} for CDD; and W m^{-2} decade^{-1} for ERF.

https://doi.org/10.5194/acp-2019-1209
Preprint. Discussion started: 4 February 2020

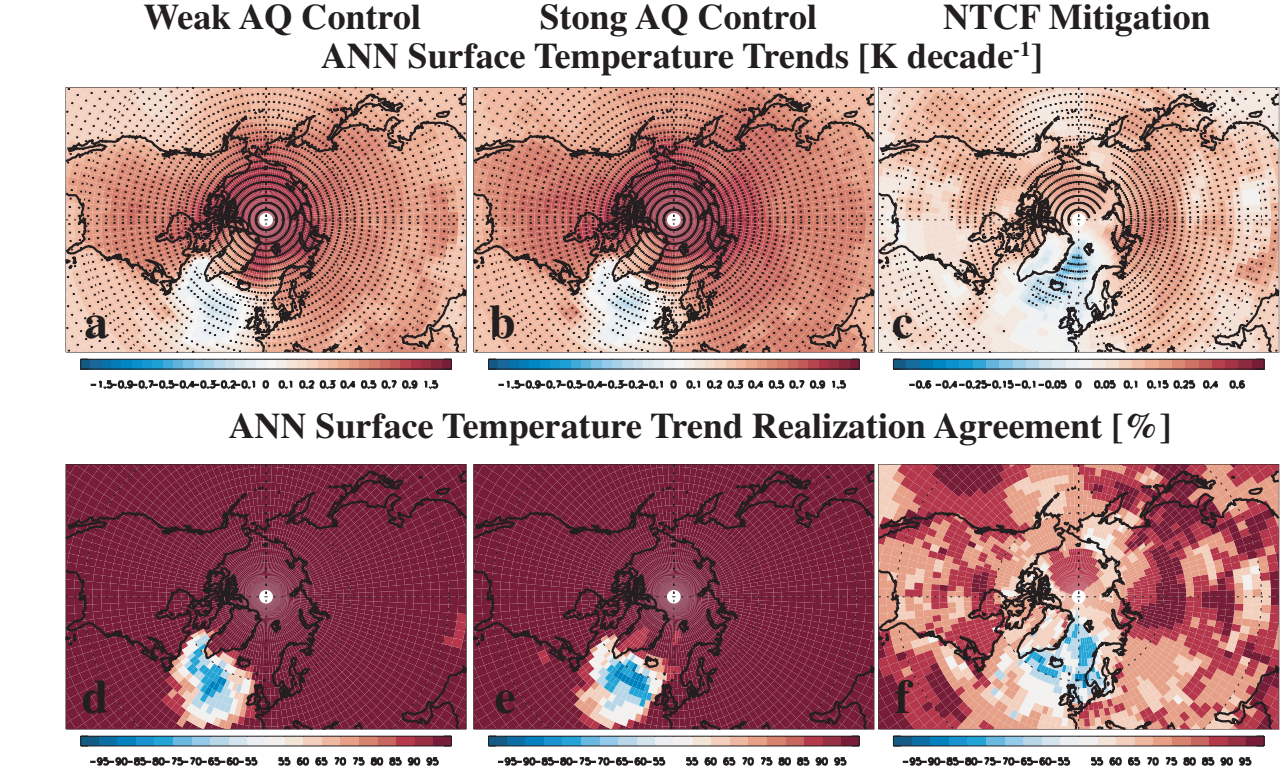

Figure 6. 2015-2055 annual mean surface temperature trends and model trend realization agreement over the Arctic. Surface temperature (a-c) trends [K decade^{-1}] and (d-f) model trend realization agreement [%] for (left panels) weak air quality control (SSP3-7.0); (middle panels) strong air quality control (SSP3-7.0-lowNTCF) and (right panels) NTCF mitigation (SSP3-7.0-lowNTCF-SSP3-7.0). Stippling denotes trend significance at the 95% confidence level based on a standard t-test. Trend realization agreement represents the percentage of models that agree on the sign of the trend.

https://doi.org/10.5194/acp-2019-1209
Preprint. Discussion started: 4 February 2020

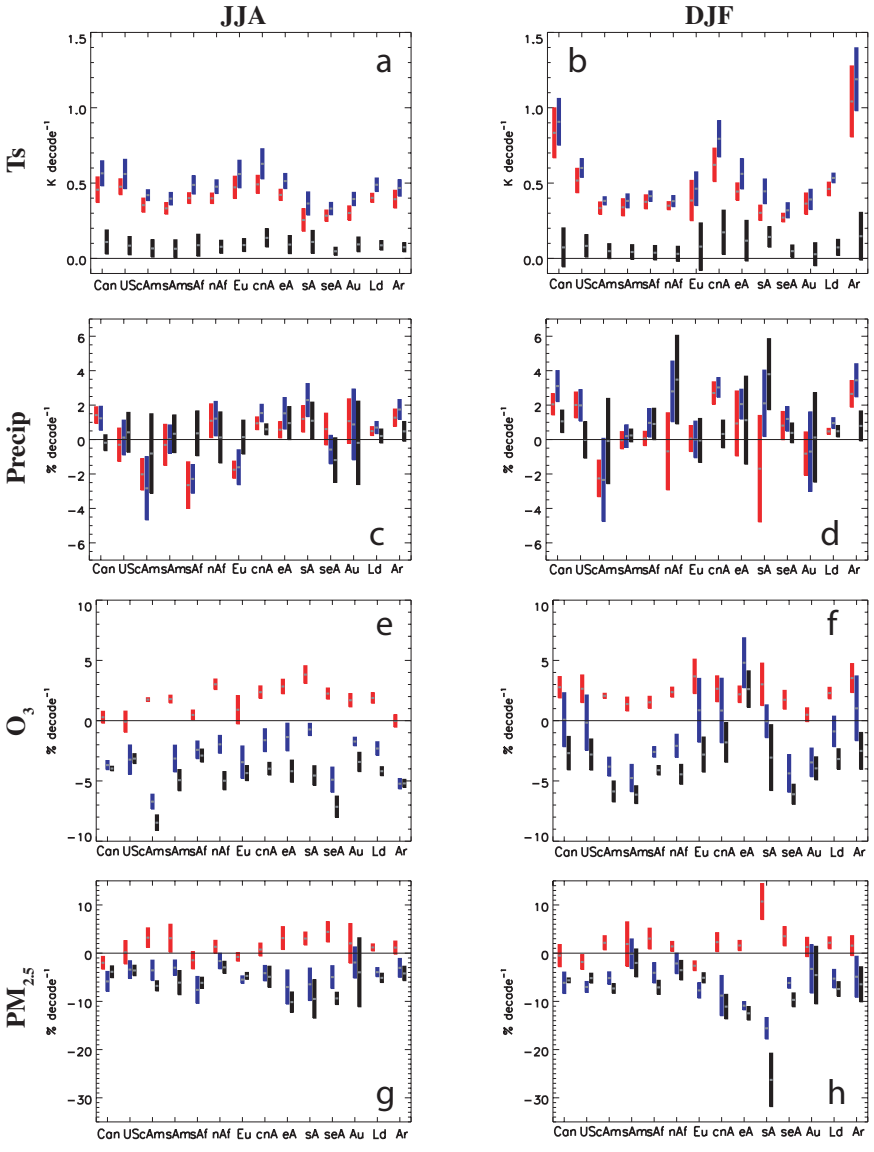

Figure 7. Regional climate and air pollution seasonal responses to NTCF mitigation. Bar plots show regional 2015-2055 June-July-August (JJA; left panels) and December-January-February (DJF; right panels) trends in (a-b) surface temperature (T_s); (c-d) precipitation (Precip); (e-f) surface ozone (O_3); and (g-h) surface particulate matter ($PM_{2.5}$) for weak (SSP3-7.0; red) and strong (SSP3-7.0-lowNTCF; blue) air quality control, and the difference between the two scenarios (NTCF mitigation; SSP3-7.0-lowNTCF−SSP3-7.0; black). Bar center (gray horizontal line) shows the multimodel mean. Bar length represents the trend uncertainty, estimated as $2\sigma/\sqrt{n}$, where σ is the standard deviation of the trends and n is the number of models. World regions are identical to those in Figure 5. Trend units are K decade^{-1} for T_s and % decade^{-1} for Precip, $PM_{2.5}$ and O_3.

https://doi.org/10.5194/acp-2019-1209
Preprint. Discussion started: 4 February 2020

Atmospheric Chemistry and Physics Discussions

Table 1. Climate and air pollution responses to NTCF mitigation. Annual mean 2015-2055 trends in surface temperature (T_s), precipitation (Precip), hottest day, wettest day, consecutive dry days (CDD), surface particulate matter ($PM_{2.5}$) and ozone (O_3), and the effective radiative forcing (ERF) for NTCF mitigation (SSP3-7.0-lowNTCF−SSP3-7.0). First set of numbers is the global mean trend; second set of numbers is the land only trend. Trends significant at the 95% confidence level are denoted by bold font based on a *t*-test. Trend units are K decade^{-1} for T_s and hottest day; % decade^{-1} for Pr, wettest day, $PM_{2.5}$ and O_3; days per year decade^{-1} for CDD; and W m^{-2} decade^{-1} for ERF. Percent change is based on comparing the 2015-2055 trend to the 2000-2014 climatology. MMM is the multi-model mean and the last row "MMM Total" shows the total change over the entire 2015-2055 time period. The first five models include both aerosol and ozone changes (lowAERO3 models); bottom three models include only aerosol changes (lowAER models). For CESM2, which we include in lowAERO3, ozone changes are based on CESM2-WACCM. O_3 for lowAER models is not included in the overall MMM and MMM total. n/a is not available.

	T_s	Precip	Hottest Day	Wettest day	CDD	$PM_{2.5}$	O_3	ERF
BCC-ESM1	**0.09/0.14**	**0.32/0.40**	**0.09/0.14**	**0.56/0.55**	**0.25**/0.40	**−3.0/−5.4**	**−3.8/−3.0**	−0.01/0.07
GFDL-ESM4	**0.07/0.08**	**0.37**/0.20	n/a	n/a	n/a	**−3.3/−6.9**	**−4.3/−3.8**	0.03/**0.13**
CESM2-WACCM	**0.09/0.11**	**0.41**/−0.17	n/a	**0.62**/0.03	0.15/0.16	**−3.2/−5.7**	**−5.0/−4.3**	**0.16/0.23**
CESM2	0.02/0.03	**0.23**/−0.10	n/a	−0.08/−0.29	−0.02/0.14	n/a	**−4.7/−4.1**	n/a
MRI-ESM2-0	**0.04/0.07**	**0.39**/0.27	**0.06/0.09**	**0.36**/0.49	0.13/0.26	**−4.6/−5.7**	**−3.7/−3.9**	n/a
MMM	**0.06/0.09**	**0.34**/0.12	**0.08/0.12**	**0.37**/0.20	0.13/0.24	**−3.5/−5.9**	**−4.3/−3.8**	**0.06/0.14**
MMM Total	0.24/0.36	1.40/0.48	0.32/0.48	1.48/0.80	0.52/0.96	−14.0/−23.6	−17.2/−15.2	0.24/0.56
CNRM-ESM2-1	**0.04/0.05**	**0.22/0.64**	**0.04/0.05**	**0.23/0.48**	0.03/0.01	**−2.3/−6.2**	0.0/0.0	**0.12/0.16**
MIROC6	0.02/0.04	**0.13**/0.39	n/a	n/a	n/a	n/a	0.0/0.0	n/a
MPI-ESM-1-2-HAM	**0.08/0.13**	**0.26**/0.43	**0.08/0.12**	0.11/0.36	−0.14/−0.05	**−3.7/−7.9**	0.0/0.0	**0.22/0.17**
MMM	**0.05/0.07**	**0.20/0.49**	**0.06/0.08**	0.17/0.42	−0.06/−0.02	**−3.0/−7.1**	0.0/0.0	**0.17/0.17**
MMM Total	0.20/0.28	0.80/1.96	0.24/0.32	0.68/1.68	−0.24/−0.08	−12.0/−28.4	0.0/0.0	0.68/0.68
Overall MMM	**0.06/0.08**	**0.28/0.25**	**0.06/0.10**	**0.31/0.28**	0.07/0.15	**−3.3/−6.2**	**−4.3/−3.8**	**0.10/0.25**
Overall MMM Total	0.24/0.32	1.12/1.00	0.24/0.40	1.24/1.12	0.28/0.60	−13.2/−24.8	−17.2/−15.2	0.40/1.00